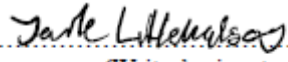
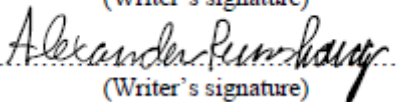




University of
Stavanger

Faculty of Science and Technology

BACHELOR'S THESIS

Study program/Specialization: Constructional engineering/	Spring semester, 2021 Open access
Writers: Litlekalsøy, Jarle Runshaug, Alexander	 (Writer's signature)  (Writer's signature)
Subject coordinator: Samarakoon, Samindi Supervisor(s): Naotunna Nilanga, Chavin and Samarkoon, Samindi	
Thesis title: Experimental investigation of crack spacing	
Credits (ECTS): 20	
Key words: <ul style="list-style-type: none">- Crack Spacing- Concrete cover thickness- Crack Width- Axial tension	Pages: 68 + supplemental material/other: 60 Stavanger, 15.05.2021. Date/year

Frontpage for bachelor thesis
Faculty of Science and Technology
Decision made by the Dean October 30th 2009

Abstract

Cracks in concrete structures have an effect on both the durability and the visuals of the structure. Therefore, it is important to control the cracks in reinforced concrete structures. This thesis address the difference in concrete cover thickness and how it affects the crack spacing and width. The concrete cover thickness is an important parameter when calculating the crack spacing and width of a reinforced concrete structure. From the Eurocode 2 and the Model Code 2010 the concrete cover is very deciding when calculating the crack spacing and width. This thesis compares the results from an experiment consisting of three different cover thicknesses against the results using the calculations from the current standards. Earlier studies suggests that the formulations in the current standards regarding the crack spacing and the crack width are questionable. The experiment for this thesis contained of testing six reinforced concrete specimens by applying axial tensile load.

Preface

First of all we would like to express our greatest gratitude to our subject coordinator Samindi Samarakoon and our supervisor Chavin Guruge. We have sincere appreciation for the guidance we have received throughout the entire process of this thesis, their help and experience have been significant all the way from the beginning until the due date. The journey has been both enlightening and demanding.

In addition, we would like to convey our thanks to chief engineer Jarle Berge and senior engineer Samdar Kakay for the assistance in the laboratory and the counselling along the way. We are also thankful for the help at IKM in Tananger and the machine laboratory at UiS for the assistance. At last, other students have helped with relevant discussions and motivation as well.

Contents

Abstract	i
Preface	ii
Contents	iii
Figures	vii
Tables	xii
Nomenclature	xiii
Table of abbreviation	xv
1 Introduction	1
1.1 Background	1
1.2 Objective	1
1.3 Overview	1
2 Literature Review	2
2.1 Importance of controlling cracks in reinforced concrete structures	2
2.2 Crack width control criteria at design stage of structure	3
2.2.1 Crack width control in EC2	3
2.2.2 Crack width control in Model code 2010	5
2.3 Crack Spacing models in literature	6

2.3.1	Bond-slip theory	7
2.3.2	No-slip theory	7
2.3.3	Saint-Venant's principle	7
2.4	Experimental investigation of cracking behavior in reinforced concrete components .	8
2.4.1	Axial tension test	8
2.4.2	Four point bending test	9
2.5	Limitations and challenges in testing methods	10
3	Materials and Methods	12
3.1	Experimental plan	12
3.2	Formwork preparation	13
3.3	Design of end connections to apply load	16
3.3.1	Changes on the steel design with increased hole-size	24
3.4	Reinforcement	24
3.5	Concrete mix design	25
3.5.1	Specimens for testing	27
3.5.2	Cubes and cylinders for testing	28
3.5.3	Volume calculations	28
3.6	Test set up at IKM	29
4	Results of the Experiment	30
4.1	Compressive test	30
4.2	Young's modulus test	31

4.3	Fracture energy - Wedge splitting test	34
4.4	Splitting tensile test	36
4.5	IKM test - Axial tensile strength. Crack spacing	39
5	Comparisons between experimental findings and literature	40
5.1	Experimental findings	40
5.1.1	IKM Test	41
5.1.2	Crack Spacing	41
5.2	Theoretical assumptions from literature	43
5.2.1	Crack spacing	43
5.2.2	Differences in cover for reinforcement	48
6	Discussion	49
6.1	Experimental investigation of crack spacing	49
6.2	Formulations from the Eurocode 2 and Model Code 2010	50
7	Conclusion	51
7.1	Recommendation for further research	52
	References	53
A	Concrete Matrix	54
A.1	Sola betong matrix	54
A.2	Superplasticizers	60
B	Test protocols	61

B.1	Young's Modulus	61
B.2	Compression test	62
B.3	Splitting tensile test	63
B.4	Applied forces at IKM	64
B.5	Crack spacing results	70
C	Order and design of load connections	76
C.1	Order of load connections	76
C.2	Design of load connections	80
D	Images of cracks in concrete	107

List of Figures

3.1	Cross section of test specimens	12
3.2	Details of the formwork	13
3.3	Formwork without reinforcement	13
3.4	Fresh concrete	14
3.5	Concrete beams covered in polyethylene	15
3.6	Beams for steel design (All dimensions are given in mm)	17
3.7	calculation of e and m	18
3.8	Grading of aggregates in concrete: Single sized, poorly sized and well-graded	26
3.9	Cast concrete for testing	28
3.10	Test set up at IKM	29
3.11	Illustration from Naotunna et AL [1]	30
4.1	Compression Test	30
4.2	Setup for wedge splitting test [2]	34
4.3	F_s - COD graph	35
4.4	Splitting tensile test	36
4.5	Splitting tensile test	38
4.6	Threaded section after surpassing maximum design resistance	40
5.1	35 mm cover	41
5.2	60 mm cover	42
5.3	85 mm cover	42

6.1	Histogram of crack spacing distribution	50
A.1	Concrete matrix	55
A.2	Concrete matrix	56
A.3	Concrete matrix	57
A.4	Concrete matrix	58
A.5	Concrete matrix	59
A.6	Dynamon SX-23 Superplasticizer	60
B.1	Young's modulus	61
B.2	Compression test	62
B.3	Splitting tensile test	63
B.4	Load applied beam 1	64
B.5	Load applied on beam 2	65
B.6	Load applied on beam 3	66
B.7	Load applied on beam 4	67
B.8	Load applied on beam 5	68
B.9	Load applied on beam 6	69
B.10	Crack spacing - beam 1	70
B.11	Crack spacing - beam 2	71
B.12	Crack spacing - beam 3	72
B.13	Crack spacing - beam 4	73
B.14	Crack spacing - beam 5	74
B.15	Crack spacing - beam 6	75

C.1	Complete order of load connections	76
C.2	Complete order of load connections	77
C.3	Complete order of load connections	78
C.4	Complete order of load connections	79
C.5	Design of 35 mm load connection part 1/9	80
C.6	Design of 35 mm load connection part 2/9	81
C.7	Design of 35 mm load connection part 3/9	82
C.8	Design of 35 mm load connection part 4/9	83
C.9	Design of 35 mm load connection part 5/9	84
C.10	Design of 35 mm load connection part 6/9	85
C.11	Design of 35 mm load connection part 7/9	86
C.12	Design of 35 mm load connection part 8/9	87
C.13	Design of 35 mm load connection part 9/9	88
C.14	Design of 60 mm load connection part 1/9	89
C.15	Design of 60 mm load connection part 2/9	90
C.16	Design of 60 mm load connection part 3/9	91
C.17	Design of 60 mm load connection part 4/9	92
C.18	Design of 60 mm load connection part 5/9	93
C.19	Design of 60 mm load connection part 6/9	94
C.20	Design of 60 mm load connection part 7/9	95
C.21	Design of 60 mm load connection part 8/9	96
C.22	Design of 60 mm load connection part 9/9	97

C.23 Design of 85 mm load connection part 1/9	98
C.24 Design of 85 mm load connection part 2/9	99
C.25 Design of 85 mm load connection part 3/9	100
C.26 Design of 85 mm load connection part 4/9	101
C.27 Design of 85 mm load connection part 5/9	102
C.28 Design of 85 mm load connection part 6/9	103
C.29 Design of 85 mm load connection part 7/9	104
C.30 Design of 85 mm load connection part 8/9	105
C.31 Design of 85 mm load connection part 9/9	106
D.1 Beam 1 - Side 1	107
D.2 Beam 1 - Side 2	107
D.3 Beam 1 - Side 3	108
D.4 Beam 1 - Side 4	108
D.5 Beam 2 - Side 1	108
D.6 Beam 2 - Side 1	108
D.7 Beam 2 - Side 3	109
D.8 Beam 2 - Side 4	109
D.9 Beam 3 - Side 1	109
D.10 Beam 3 - Side 2	109
D.11 Beam 3 - Side 3	110
D.12 Beam 3 - Side 4	110
D.13 Beam 4 - Side 1	110

D.14 Beam 4 - Side 2	110
D.15 Beam 4 - Side 3	111
D.16 Beam 4 - Side 4	111
D.17 Beam 5 - Side 1	111
D.18 Beam 5 - Side 2	111
D.19 Beam 5 - Side 3	112
D.20 Beam 5 - Side 4	112
D.21 Beam 6 - Side 1	112
D.22 Beam 6 - Side 2	112
D.23 Beam 6 - Side 3	113
D.24 Beam 6 - Side 4	113

List of Tables

1	Values for τ_{bms} , β and η_r [3]	6
2	Experimental plan	12
3	Minimum design resistance	24
4	Mixing ratio	27
5	Concrete order	28
6	Compression test	31
7	Young's modulus	33
8	WST test results	35
9	Splitting tensile test results	37
10	Splitting tensile test results from earlier test	37
11	Maximum applied force on beams at IKM	39
12	Mean values and Standard deviation of crack spacing	42

Nomenclature

Greek letters

β	coefficient to assess the mean strain over the transfer length
ϵ	Strain
ϵ_{cm}	average concrete strain over the length $l_{s,max}$
ϵ_{cs}	strain of the concrete due to shrinkage
ϵ_{sh}	shrinkage strain
ϵ_{sm}	average steel strain over the length $l_{s,max}$
η_r	coefficient considering the shrinkage
ϕ	Bar diameter
σ	Stress
σ_{sr}	maximum steel stress in a crack in the crack formation stage
σ_s	Steel stress in crack
τ_{bms}	Mean bond strength between steel and concrete
ξ	Adhesion ratio

Roman upper case letters

A_s	Effective steel area
$A_{c,eff}$	Effective concrete area
C_{nom}	Nominal concrete cover
E_s	Young's modulus for steel
E_{cm}	Young's modulus for concrete
$P_{p,eff}$	Effective steel area [EC2]

W_d Calculated crack width
 W_k Maximum crack width
 W_{lim} Recommended crack width limit

Roman lower case letters

c Concrete cover
 e Relationship between $\frac{Es}{E_{cm}}$
 $f_{ct,eff}$ Effective concrete tensile strength
 f_{ctm} Mean value of the concrete tensile strength
 $l_{s,max}$ Transfer length from crack
 $s_{r,max}$ Maximum crack spacing

Table of abbreviations

W/C	Water and cement ratio
EC2	Eurocode 2
MC2010	Model Code 2010
SP	Superplasticizers
fib	The International Federation for Structural Concrete
ULS	Ultimate limit state
SLS	Servicability limit state
DIC	Digital Image Correlation
RC	Reinforced Concrete
UiS	University of Stavanger

1 Introduction

1.1 Background

Cracks in reinforced concrete (RC) structures are controlled at the design stage by limiting the calculated crack width. Axial tensile experiments of RC ties are one of the main experiments used to develop these existing crack width calculation models. Axial tensile experiments are commonly done with RC specimen with a single reinforcement. However, it has been identified that such experiments are unable to simulate the actual behaviour of RC members in practice. Therefore, researchers are currently focusing on axial tensile experiments with several numbers of reinforcement bars. These experiments require special testing rigs which are available at the IKM laboratory in Tangerang. Conducting an axial tensile experiment with multiple reinforcement bars allows identifying the behaviour of crack governing parameters in RC members. Results of such experiments can be used to improve the existing crack width calculation models.

1.2 Objective

The objective of this thesis is to study the effect of concrete cover on the cracking behaviour in reinforced concrete structures. In this study, the concrete cover thickness 35mm, 60mm and 85mm has been studied.

1.3 Overview

The thesis is divided into 7 chapters. The first chapter consists of an introduction and provides the background. The second chapter contains the literature review and the crack spacing and crack width models are introduced in this chapter. The third chapter explains materials and methods used for the experiments. The results are presented in the fourth chapter, while the comparisons between the experimental findings and literature appear in chapter five. Respectively, the discussion and conclusion are found in chapters six and seven.

2 Literature Review

2.1 Importance of controlling cracks in reinforced concrete structures

Controlling the cracks in reinforced concrete is important and necessary in order to handle issues concerning the durability and the visuals of the concrete. Larger cracks in the concrete would affect the visual presentation for the public, and make them believe there is a structural problem that can lead to danger. In general, cracks in reinforced concrete will often lead to issues with either the durability of the concrete or the reinforcement. Cracks allows water to enter the concrete which may lead to mechanical weathering. Other factors as oxygen and chloride, in the same way as water, may reach the reinforcement in the concrete and may cause deterioration and corrosion.

When cracks occur in the concrete, the reinforcement is forced to carry the tensile force. The compressive strength of the concrete is estimated to be ten times larger than the tensile strength. With reinforced concrete we have both compressive and tensile strength. As mentioned, cracks can affect the durability and the strength of the concrete. According to research, the concrete will not be endangered if these factors are present:

1. Small crack widths
2. Concrete cover of the reinforcement is sufficient
3. The mixture composition of the concrete meets requirements regarding durability and strength

When designing a normal concrete structure, the crack width limitation will not decide how the concrete will be designed. The crack width is important when the structure is designed to places with for example tough environmental conditions, or when there is a low reinforcement ratio.

2.2 Crack width control criteria at design stage of structure

The current standards do not clearly define the concepts of mean, characteristic and maximum values, regarding the crack spacing and the crack width. This lack of definition can cause problems for their users. The verification equation for the crack width is written below: [4]

$$W_d \leq W_{lim}$$

Where W_d is the characteristic crack width and W_{lim} denotes the nominal limit value of the crack width considered at the concrete surface. [4]

The design value from the current standards is either a maximum characteristic value or the value is very close to the maximum. The issue with this value is that it does not impact the safety of the structure, but it is used for verification purposes in serviceability limit states. From the studies of Barre et al.(2016) [4], it is mentioned that this approach is not desirable when the water- or air-tightness requirements must be justified, fulfilled or equivalent. [4]

2.2.1 Crack width control in EC2

The calculations of crack width from the Eurocode 2 are mainly focused on the formation of cracks for a longer period of time. From the Eurocode 2 the crack width (W_k) can be found by multiplying the maximum crack spacing with the mean difference of the strain in the reinforcement bar (ϵ_{sm}) and the strain in the concrete (ϵ_{cm}). [5]

$$W_k = S_{r,max}(\epsilon_{sm} - \epsilon_{cm})$$

The mean stress difference between the reinforcement and the concrete can be calculated like this:

$$\epsilon_{sm} - \epsilon_{cm} = \frac{\sigma_s - k_t \frac{f_{ct,eff}}{P_{p,eff}} (1 + \alpha_e P_{p,eff})}{E_s}$$

σ_s - stress in the tensile reinforcement assuming an elevated cross section.

e - relationship between E_s / E_{cm}

E_s - Young's modulus for steel

E_{cm} - Young's modulus for concrete

$P_{p,eff}$ - reinforcement ratio, defined by $\frac{(A_s + \xi 1 A_p)}{(A_{c,eff})}$

Where $A_{c,eff}$ is the effective area of the concrete tensile zone that surrounds the reinforcement A_p is the area of pre-stressed or post-stressed rebars in the effective area $A_{c,eff}$.

ξ_1 - the adhesion ratio defined by: $\frac{\xi \phi s}{\phi p^{(0.5)}}$

k_t - is a factor that depends on the loads duration

$k_t = 0.6$ for short-term load

$k_1 = 0.4$ for long-term load

One of the main factors when calculating the crack width is the maximum crack spacing, $s_{r,max}$. The maximum crack spacing is defined by factors as the bar diameter (ϕ), the concrete cover (c) and the effective steel area ($P_{p,eff}$). The magnitude of the impact of the cover concrete and reinforcement bar is determined by four different constants: k_1, k_2, k_3 and k_4 .

$$s_{r,max} = k_3 c + \frac{k_1 k_2 k_4 \phi}{p_{p,eff}}$$

k_1 - 0.8 with ribs on the bar and 1.6 without ribs

k_2 - Load distribution: 0.5 for bending and 1.0 for axial tension

k_3 - Cover impact: 3.4 recommended by NS-EN 1992-1-1

k_4 - Reinforcement bar impact: 0.425 recommended by NS-EN 1992-1-1

2.2.2 Crack width control in Model code 2010

The characteristic crack width is determined by the maximum transfer length and the relative mean strain. The maximum crack spacing $s_{r,max}$ from Eurocode 2 is related to the transfer length in the Model Code 2010 and can be understood like this: $2l_{s,max} = s_{r,max}$ [4] The crack width is defined by:

$$W_d = 2l_{s,max}(\epsilon_{sm} - \epsilon_{cm} - \epsilon_{cs})$$

ϵ_{sm} - average steel strain over the length $l_{s,max}$

ϵ_{cm} - average concrete strain over the length $l_{s,max}$

ϵ_{cs} - strain of the concrete due to shrinkage

The equation can be rewritten for calculating crack width under bending and tensile cases:

Axial tension: $W_d = 2l_{s,max}\epsilon_m$

Bending: $W_d = 2l_{s,max}\epsilon_m F$

ϵ_m - mean strain difference of steel and concrete

The $l_{s,max}$ can be found by the equation below:

$$l_{s,max} = k * c + \frac{1}{4} * \frac{f_{ctm}}{\tau_{bms}} * \frac{\phi s}{P_{s,ef}}$$

The mean strain difference is defined by the equation below:

$$\epsilon_{sm} - \epsilon_{cm} - \epsilon_{cs} = \frac{\sigma_s - \beta * \sigma_{sr}}{E_s} - \eta_r * \epsilon_{sh}$$

σ_s - steel stress in the crack

σ_{sr} - maximum steel stress in a crack, in the crack formation stage, defined by the equation below:

$$\sigma_{sr} = \frac{f_{ctm}}{P_{s,ef}} (1 + \alpha_e P_{s,ef})$$

$$P_{s,ef} = \frac{As}{A_{c,eff}}$$

α_e - is the modular ratio = E_s/E_c

β - is an empirical coefficient to assess the mean strain over the transfer length decided by the table below

η_r - coefficient considering the shrinkage

ϵ_{sh} - shrinkage strain

	Crack formation stage	Stabilized cracking stage
Short term, instantaneous loading	$\tau_{bms} = 1.8 * f_{ctm}(t)$ $\beta = 0.6$ $\eta_r = 0$	$\tau_{bms} = 1.8 * f_{ctm}(t)$ $\beta = 0.6$ $\eta_r = 0$
Long term, repeated loading	$\tau_{bms} = 1.35 * f_{ctm}(t)$ $\beta = 0.6$ $\eta_r = 0$	$\tau_{bms} = 1.8 * f_{ctm}(t)$ $\beta = 0.4$ $\eta_r = 1$

Table 1: Values for τ_{bms} , β and η_r [3]

3.8

As shown, the calculations from the Eurocode 2 and the Model Code 2010 are respectively similar. An important parameter in both standards are the maximum crack spacing, or the maximum transfer length. It is clear that in both cases the cover of the concrete is crucial for the calculations of the crack spacing and later the crack width.

2.3 Crack Spacing models in literature

Over the recent years many studies have been done to examine the behaviour of the crack spacing and width. Recent studies have identified that crack spacing increases with the concrete cover, both in flexure and axial tension. Many of these studies have been conducted to identify the effect of the reinforcement layout. [1] Through these studies we learn that researchers are disagreeing on certain parameters. For example Rimkus et al.(2019) [6] have concerns regarding the correlation between the width of the crack and the ratio $\phi/p_{p,eff}$ and if the characteristics of the reinforcement have any impact on the crack width at all. Other researchers, like Tan et al.(2018) [7] think that the characteristics of the reinforcement probably should play a bigger role in the calculations from the EC2 and the MC2010. For this thesis, there were conducted experiments with only one size in the

bar diameter. There seems to be very few questions from researchers about the importance of the concrete cover, but the recent studies are debating whether or not the calculations from the current standards are sufficient in the design stage of the structure. [6] [7]

2.3.1 Bond-slip theory

The bond-slip theory was first introduced by Saliger in 1936 [1], and this theory addresses how the concrete behaves when there is a slip between the reinforcement and concrete. The slip will be largest at the crack and decreases when moving further away from the crack. Because of the slip, the concrete strain is different to the strain in the reinforcement. When there is no slip between two cracks, the strain in the concrete and the reinforcement can be considered similar. [1]

2.3.2 No-slip theory

Broms first introduced the no-slip theory in 1965 [1], and unlike the bond-slip theory it is assumed that there is no slip between the concrete and the reinforcement. With the assumption that there is a perfect bond, no slip, between the concrete and the reinforcement, the crack width will in theory be zero at the reinforcement. The stress is spreading when moving away from the crack, and the distance from the crack to where the uniform stress distribution of the concrete specimen becomes proportional to the concrete cover thickness. [1]

2.3.3 Saint-Venant's principle

The principle of Saint-Venant, after Jean Claude Barré de Saint-Venant, is a principle regarding statistically equivalent loads. With a distance isolated from the region where the load is applied, the stress and strain in the body will be uniform for any boundary condition, as long as it is an equivalent resultant load. Naotunna et al.(2020) [1] compares the no-slip theory and Saint-Venant's principle. The uniform stress distribution of the concrete specimen becomes proportional to the concrete cover thickness. [1]

2.4 Experimental investigation of cracking behavior in reinforced concrete components

The experiment for this thesis is conducted by applying axial tensile load onto a concrete specimen with four reinforcement bars. The investigation for this experiment is to check the cracking behaviour in reinforced concrete components with different cover thickness.

2.4.1 Axial tension test

Usually, the axial tension tests are executed with a single reinforcement bar and often shorter specimens. With this type of experiment it has been experienced that there will be produced fewer cracks. With that in mind, the experiment conducted for this thesis tests larger specimens with four reinforcements bar. By using 2000-mm-length specimens there will be generated more cracks with more data of crack spacing. To generate more cracks the specimens were designed to have a lower concrete cover thickness and a higher effective steel area. For this thesis, there were conducted experiments on specimens with various concrete cover thickness to observe the behaviour of crack spacing with different cover thicknesses. Therefore, six specimens of 300mx300mx2000mm were cast with two specimens of each of these cover thicknesses; 35mm, 60mm and 85mm. The specimens were cast with four 32-mm-diameter bar and they were threaded to fit with M24 nuts. The form work was made to keep the reinforcement in place to get the right cover thickness. Due to the large specimens, the axial tension test could not be completed with a conventional displacement-controlled testing machine. Therefore, the specimens were shipped to the IKM Laboratory in Tananger, Norway where the tensile load could be applied with a "force-controlled" bench. This made it possible to control the tensile force applied to the specimens, and it was decided to increase the load in 100kN steps. The load was applied to the reinforcement, through the nut and bolt mechanism. Since the reinforcement bars were cut to be 2500mm long, the load connections was made from a standard HEB S355 1000 beam that was cut to fit the specimens. To connect the load connection to the specimen, holes were drilled for the reinforcement and one hole for the connection to the testing bench on each side. As explained later in the thesis, the load connections were designed and checked for it to handle the tensile, shear and tear-out failure modes separately. From the calculations shown later in the thesis, the load connections should withstand a load of 90 tons.

2.4.2 Four point bending test

Four point bending test, often called four point flexural test, is often used on brittle materials, such as concrete. The test is used in order to determine different properties of the concrete. From the test properties such as Modulus of elasticity in bending E_f , flexural stress σ_f and the flexural strain ϵ_f . From the results the stress-strain response from the material can be found. The four point bending test was not performed for this thesis due to lack of materials.

2.5 Limitations and challenges in testing methods

During the entire process we happened upon a large variation of problems. Early during the process the largest difficulties were to find different literature and simply understanding the topic, but we have also faced some practical issues. Instead of ordering the form work, we had to make it from scratch. As we have explained later during methods we had to make the design cost efficient combined with the pressure on time. Because of the time it would take, we had to focus on the practical before the theoretical.

When we had finished the form work for the six beams, we ordered the concrete. From a previous project we had 12 of the rebars. The other 12 had to be threaded at the machine lab at UiS. There were slight issues during the threading procedure. Because of the size, it had to be manually threaded. During the concrete process we did not have any issues. During the hardening process we could do the steel connection design, as well as starting the theoretical work. The steel design was also quite forward. Due to the pandemic, most of the work had to be done from home. Gaining access to the correct standards for the calculation did produce some minor issues.

After the concrete was hardened and the steel parts arrived. We could finally check the load connections on the reinforced concrete beams. Some displacements in the reinforcement due to the form work in combination with some displacement of the holes in the load connection, led to them not fitting. We had to manually increase the sizes of the holes on the load connections. After the holes was made larger, the increased dimensional movement helped so the load connections would work. When everything were in place we went to the IKM laboratory in Tananger in order to do the axial tensile strength tests. The day before the tests we prepared the LaVision DIC system in order to do the crack width and stress analysis. During the tests, there were no major issues. As calculated, the steel parts would malfunction before the concrete at a force around 90 kilo-newton, depending on the concrete cover.

After the tests were completed at IKM, the data-set were used to analyze the stress/strain and the crack width with the DIC. Problems were encountered during this process. Due to several issues, the DIC did not work appropriately. The main problem was the calibration of the software that was done during the tests. Throughout the test, it did not seem like there was any problems with the calibration. The problems were first encountered when starting the analyzing part. This may have occurred for several different reasons. After conversations with the LaVision correspondent, the main problem from our dataset is the angle from the camera towards the test specimen. On

account of the test set up at IKM, there were not any suitable ways to get a proper data set. In combination with the lack of lighting and some inadequate speckle pattern, the analysis could not be accomplished. Without the DIC analysis we could not investigate the experimental crack width as well as the stress and strain in the specimens at the maximum applied tensile load.

During the testing of the concrete some complications occurred. With the fresh concrete, there were no opportunities to carry out the slump test, nor the air content test. This was because of a lack of sufficient time and materials at the specific day. These tests must be done while the concrete is fresh and with the same concrete batch our specimens were made from. The slump test would verify the workability of the concrete, as well as to see if it has a correct amount of water in the concrete mix. The air content is measured in percent. The amount of air in the concrete affects the characteristics of the concrete. During the testing of the hardened concrete specimens, some more obstacles took place. As discussed later during the results of the experiments, a number of two test specimens for each test might not be enough to verify the results. With at least three or more specimens, an uncommon result could be neglected. Comparing the test results from our specimens with other students, we can get some understanding whether the results are acceptable or not. During the Young's Modulus test, there have been complications for all students that have finished the test.

After all the tests were completed, the crack spacing had to be measured manually. Insufficient tools to measure the cracks may cause some inaccuracies. With the naked eye, most cracks were not possible to see. With the help of a microscope from Ivar Langens at UiS, the cracks could be seen and marked to some extent.

3 Materials and Methods

3.1 Experimental plan

The experimental plan of this project is based on a lot of practical work in advance of the tests. First of all, the reinforcement and formwork had to be ready before the concrete casting. The table below shows the objectives for the experiment and when they were due. From the table, it is noticeable that the reinforcement and formwork had to be done by 28.02.2021 in order to complete the concrete casting in time. Since the concrete needed at least 28 days to harden, it was crucial that the objectives prior were completed.

Task/Test	Machines and Instruments	Due date
Reinforcement threading	Machine Lab UiS	28.02.2021
Formwork	Tools from Ivar Langens Hus	28.02.2021
Concrete casting	Concrete truck at Ivar Langens Hus	09.03.2021
Load connections	Tools from Machine Lab UiS	09.03.2021
Compressive test	Test apparatus at Ivar Langens Hus	17.03.2021
Young's modulus test	Test apparatus at Ivar Langens Hus	17.03.2021
Splitting tensile test	Test apparatus at Ivar Langens Hus	17.03.2021
Fracture energy test	Test apparatus at Ivar Langens Hus	26.03.2021
Main test	"Force-controlled" bench at IKM Tananger	09.03.2021
Crack width and strain management	DIC Instrument	09.03.2021

Table 2: Experimental plan
3.8

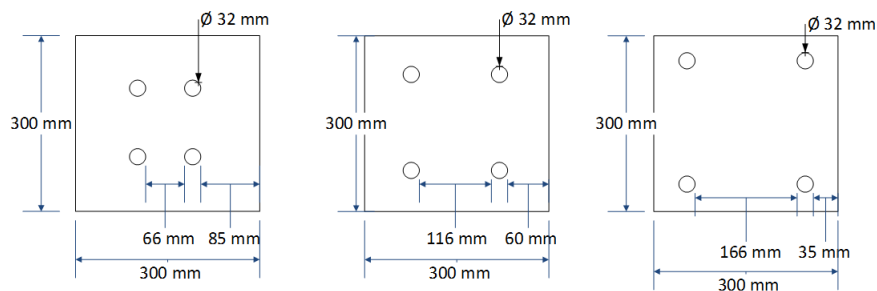


Figure 3.1: Cross section of test specimens

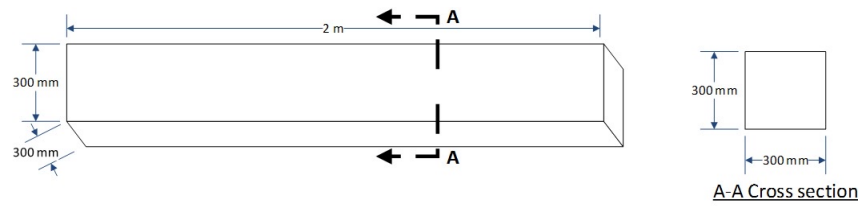
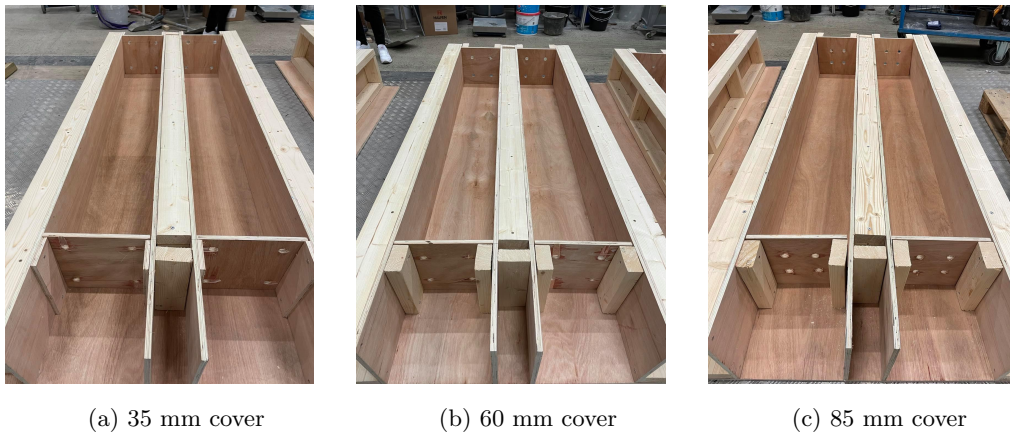


Figure 3.2: Details of the formwork

3.2 Formwork preparation

To cast all six specimens at once, it was necessary to make formwork for all of them. Wood was used as the material for the formwork. When using wood as formwork, it is easier to shape it and it is easier to disassemble after the concrete has hardened. For the project it was required six formworks with dimension 300x300x2000mm. As seen in the figure 3.3 the holes made for the rebars were made in the formwork. The reinforcement will be inside the formwork before the casting of the concrete specimens.



(a) 35 mm cover

(b) 60 mm cover

(c) 85 mm cover

Figure 3.3: Formwork without reinforcement



(1) Fresh concrete 35 mm



(2) Fresh concrete 60 mm



(3) Fresh concrete 85 mm

Figure 3.4: Fresh concrete

During the casting, the fresh concrete was tamped with several strokes in order to compact the concrete. Without compacting the concrete there might be places that is not completely filled within the formwork. It is important to not compact too much as well, because there should be some air in the concrete mix. Inadequate compacting can cause honeycombing in the concrete. This is done in order to improve the settling rate of the concrete. After the concrete specimens reached the point seen in the pictures above in figure 3.4, the concrete was covered in polyethylene as shown in figure 3.5 in order to keep the moisture in the concrete during the hardening process.

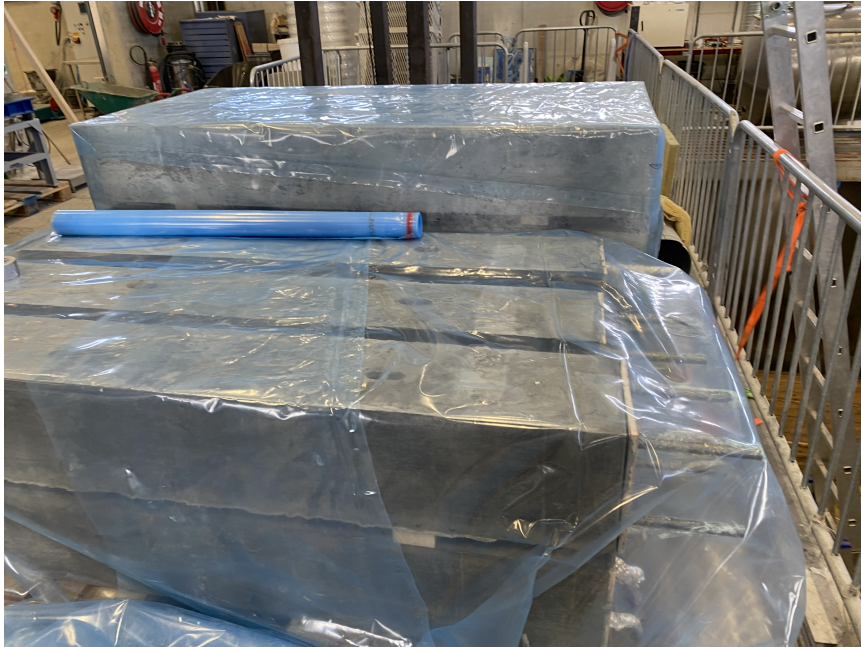


Figure 3.5: Concrete beams covered in polyethylene

3.3 Design of end connections to apply load

HEB beams with specific requirements was ordered from Norsk Staal in order to make the load connections. HEB 1000 beams were chosen for economical reasons and the beams characteristics. HEB has a greater load capacity than HEA beams. In regards to cost efficiency, both sides will be used. From Norsk Staal, HEB 1000 beams were available with S355 steel strength. The experiment demanded that the load connections would sustain a large amount of tensile forces. Beneficially, the maximum resistance of the steel connections were calculated in order to know what quantity of loading we can expose the beams at IKM.

The cross-section below in figure 3.6 shows the different measurements on the beams for the steel design. Some of the properties will be the same on the different load connections, as all of the connections are made with HEB 1000 beams with S355 steel strength. The steel design for all three concrete cover sizes is shown in the appendix. Some calculations are similar on all three cover sizes, and are therefore kept in the design below.

Sectional properties of HEB section

$$t_w = \text{thickness web} = 19 \text{ mm}$$

$$t_f = \text{thickness flange} = 36 \text{ mm}$$

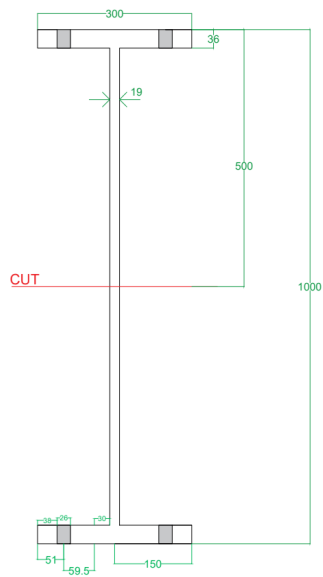
$$h_w = \text{height web} = 450 \text{ mm}$$

$$l_f = \text{length flange} = 300 \text{ mm}$$

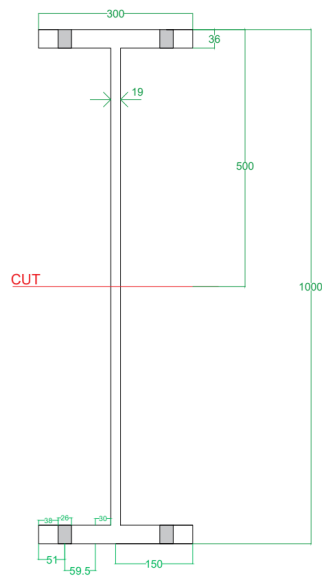
$$f_y = \text{Yield strength of web and flange} = 355 \frac{N}{mm^2} \text{ [EN 1993 1.1 Table 3.1]}$$

$$f_{y_{bolt}} = \text{Yield strength of bolt section} = 500 \text{ N/mm}^2$$

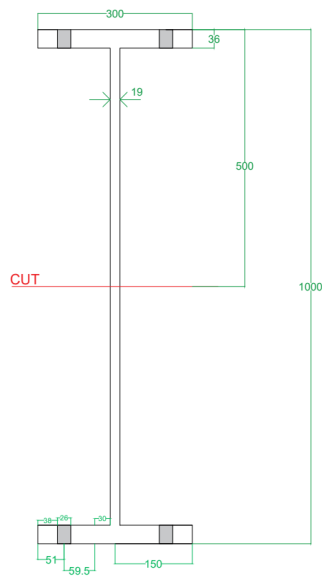
The bolt is the threaded section



(1) 35 mm concrete cover



(2) 60 mm concrete cover



(3) 85 mm concrete cover

Figure 3.6: Beams for steel design (All dimensions are given in mm)

Resistance of T-Stubs - Step 1A The following parameters/values are calculated as shown in NS EN 1993 1.8 [8] Table 6.2 and the figure 3.7 below from the same standard.

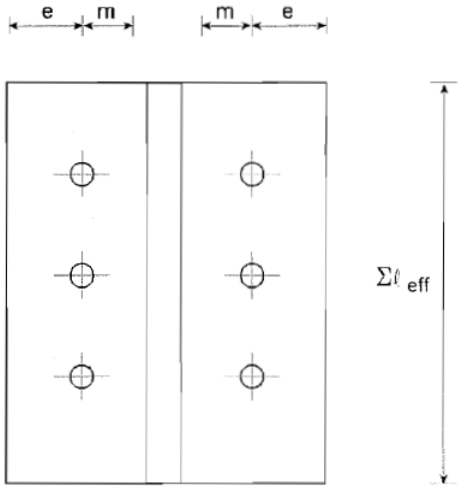


Figure 3.7: calculation of e and m

For a circular failure pattern

$$\begin{array}{l|l} \text{End} & l_{eff,1} = 2 * \pi * m_1 \\ \text{bolt} & l_{eff,11} = \pi + 2 * e_1 = \end{array}$$

For a non-circular failure pattern

$$\begin{array}{l|l} \text{End} & l_{eff,2} = 4 * m_1 + 1.25 * n \\ \text{bolt} & l_{eff,22} = 2m_1 + 0.625 e_1 + e_1 \end{array}$$

$$ew = \frac{dw}{4} = \frac{41.6mm}{4} = 0.01 \text{ m}$$

$$\gamma M0 = 1$$

$$\gamma M1 = 1$$

$$d_{boltm} = \frac{24.84mm + 23.16mm}{2} = 0.024 \text{ m}$$

$$FtRd = \pi * \left(\frac{d_{boltm}}{2}\right)^2 * f_{ybolt} = 226.08 \text{ kN}$$

The lesser value of $l_{eff,1}$ and $l_{eff,11}$ must be chosen

$$M_{pl,1}Rd = \frac{0.25 * l_{eff,11} * t^2 * fy}{\gamma M0}$$

Use the lesser value of $l_{eff,2}$ and $l_{eff,22}$

$$M_{pl,2}Rd = \frac{0.25 * l_{eff,22} * t^2 * fy}{\gamma M0}$$

Mode 1 failure: Complete flange yielding

$$Ft_1Rd = \frac{(8 * n - 2ew) * M_{pl,1}Rd}{2 * m_1 * n - ew * (m_1 + n)}$$

Mode 2 failure: Bolt failure with flange yielding

$$Ft_2Rd = \frac{2 * M_{pl,2}Rd + n * FtRd * 4}{m_1 + n}$$

Mode 3 failure: Bolt failure

$$F_{t3}R_d = 4 * F_{tR_d}$$

Resistance of flange

Minimum of $F_{t1}R_d$, $F_{t2}R_d$ and $F_{t3}R_d = F_{t2}R_d$

Check for beam web tension - Step 1B

$$b_{effweb} = 300 \text{ mm} - 86 \text{ mm} = 0.214$$

$$t_w b = t_w = 19 \text{ mm}$$

$$f_{yb} = 355 \frac{N}{mm^2}$$

EN1993 1.8 in equation 6.22 [8]

$$F_{t_{wb}}R_d = \frac{b_{effweb} * t_w * f_{yb}}{\gamma M_0}$$

Shear failure can occur at the loading at the loading shackle connection [9]

$$A_{shear} = 2 * 257 \text{ mm} * t_w$$

$$f_{shear} = 0.6 * f_{yb}$$

$$F_{shear}R_d = A_{shear} * f_{shear}$$

Tearout failure of web [9] Tear-out is a type of shear stress. The tear-out affects the material around the hole instead of the bolt or the shackle. In order to prevent a tear-out failure, the hole must be design with a sufficient distance to the end.

Nut strength verification

The bolt is considered as the threaded end of the reinforcement and the nut is selected as M24 with strength class 8

Tensile strength of four bolt set: $F_{t3}R_d = 4 * F_{tR_d}$

Verification for the thread stripping before tensile failure of bolts.

Tensile strength of one bolt: $F_{t_{bolt}} = \frac{F_{t3}R_d}{4}$

Shear strength of bolt from reinforcement: $F_{shear,bolt} = 0.85 * f_{y,bolt}$

0.85 is the EC2 factor used when calculating shear links

Calculation of effective length:

$$A_{shear,bolt} = \frac{F_{t,bolt}}{F_{shear,bolt}}$$

$$L_{eff,shear} = \frac{A_{shear,bolt}}{\pi * d_{bolt,m}}$$

In order to hold the tensile strength of a bolt required length is

$$L_{eff,shear}$$

Thread stripping strength of bolt (Reinforcement) $F_{thread,bolt}$

Length of engagement

$$L_{eng} = 0.75 \text{ mm} * 24 \text{ mm} \text{ [Assuming only one nut is used.]}$$

$$A_{eng,shear} = \pi * d_{bolt,m} * L_{eng}$$

$$F_{thread,bolt} = A_{eng,shear} * F_{shear,bolt}$$

Thread stripping does not occur before the tensile strength of bolt

Verification for the thickness of flange (Steel plate connected to bolts)

Tensile strength verification

$$d_{bolt,m} = 0.024$$

$$r_{bolt,m} = \frac{d_{bolt,m}}{2} = 0.012 \text{ m}$$

Stress area in bottom face of steel plate (A_{bottom})

$$d_{bottom} = d_{bolt,m} + 2 * 3.5 \text{ mm} + 2 * tf$$

$$r_{bottom} = \frac{d_{bottom}}{2}$$

$$A_{bottom} = \pi * (r_{bottom}^2 - r_{bolt,m}^2)$$

Stress area in bottom face of steel top (A_{top})

$$d_{top} = d_{bolt,m} + 2 * 3.5 \text{ mm} + 2 * tf$$

$$r_{top} = \frac{d_{top}}{2}$$

$$A_{top} = \pi * (r_{top}^2 - r_{bolt,m}^2)$$

Mean tensile area ($A_{t,mean}$)

$$A_{t,mean} = \frac{A_{top} + A_{bottom}}{2}$$

Maximum possible tensile capacity of plate at single nut nut-bot ($Ft_{plate,1}$)

$$Ft_{plate,1} = fy * A_{t,mean}$$

Maximum possible tensile capacity of plate at 4 nut-bot ($Ft_{plate,4}$)

$$Ft_{plate,4} = 4 * Ft_{plate,1}$$

Shear strength verification

$$r_{shear} = r_{bolt,m} + 3.5 \text{ mm} + \frac{tf}{2}$$

Shear area

$$A_{shear,m} = 2 * \pi * r_{shear} * tf$$

Shear capacity of a single nut ($F_{shear,1}$)

$$F_{shear,1} = F_{shear} * A_{shear,m}$$

Shear capacity of four nuts $F_{shear,4}$

$$F_{shear,4} = 4 * F_{shear,1}$$

Verification for the residual stresses that may occur at the web-flange section [10]

Minimum thickness when hot-rolling

$$t_{min} = t_w = 19\text{mm}$$

Assume the maximum load per single section

$$F_{app,1} = F t_3 R_d$$

Additional tensile stress due to residual stress at the joint.

$$f_{residual} = 0.3 f_y$$

Tensile residual force at the joint. Take the length along the joint.

$$F_{residual} = t_{min} * 300 \text{ mm} * f_{residual}$$

Total applied force with residual force

$$F_{tot} = F_{app,1} + F_{residual}$$

Tensile strength of the section. Take the length along the joint. NOT at the weakest point where the shackle hole is located

$$F_{max,1} = t_{min} * 300 \text{ mm} * f_y$$

The critical point for the load connections are the threaded section of the reinforcements. As seen in the calculations, it is failure mode 2 and 3 that gives the minimum force resistance.

Concrete cover	Design hole diameter	Resistance of flange	Web tensile capacity
35 mm	26 mm	837.6 kN	1443 kN
60 mm	26 mm	904.3 kN	1443 kN
85 mm	26 mm	904.3 kN	1443 kN
35 mm	28 mm	837.6 kN	1443 kN
60 mm	28 mm	904.3 kN	1443 kN
85 mm	28 mm	904.3 kN	1443 kN

Table 3: Minimum design resistance

With the 35 mm concrete cover, the bending of the flange is also a critical part. With 60 mm and 85 mm concrete cover, the affect from the flange bending does not affect the design resistance at a significant value. This is shown in the calculations, as failure mode 3 (Bolt failure) is the case for 60 and 85 mm cover, while failure mode 2 (bolt failure with flange yielding) is the case for 35 mm concrete cover.

3.3.1 Changes on the steel design with increased hole-size

The parameters affected by the increased hole size is not one of the critical parts of the load connection. The verification for the flange thickness is affected by the diameter of the holes. The strength of the nut/washer also changes depending on the hole size. As the table 3 shows above, the theoretical maximum load the threaded reinforcement can withstand is 84 tonnes for the 35 mm concrete cover, and 90.8 tonnes for the 60 mm and the 85 mm concrete cover.

3.4 Reinforcement

The most commonly used reinforcement are steel bars, also known as rebars. The purpose of the reinforcement is, as earlier mentioned, to improve the tensile strength of the element. The surface of the steel reinforcement bars are often made with ribs, lugs or indentations in order to create a better bond with the concrete. The rebars is embedded into the form work before the concrete is cast. The rebars are held in place by extra materials. When pouring the concrete, it is important that the rebars stays in place. During the hydration process the concrete will harden with the reinforcement in the correct position. Initially, the concrete is subject to all the loading. When the cracks occur, the reinforcement will be taking the tensile load.

The steel reinforcements was ordered from the UiS Machine Lab. The steel grade of the reinforcement was B500NC. In order to complete the test with six specimens there had to be a total of 24 steel bars, 4 in each specimen. The steel bars were threaded to $\text{Ø}25$ to fit the M24 nuts. 12 bars were ordered from the Machine Lab, with a length of 2350mm where it is threaded 175mm in each end. The part of the steel bars that will be covered by concrete have a $\text{Ø}32$ diameter. 24 steel bars with $\text{Ø}32$ mm, 4 in each specimen, model.

3.5 Concrete mix design

From early on, concrete has been one of the most used building materials in the world, but it has grown significantly in the last 200 years. The use of concrete is diverse and it can be found in smaller constructions like pavement and fences, but also in larger constructions like skyscrapers, power plants and dams. Concrete is versatile and it has no constraints when it comes to shape and size. Concrete is a composition of aggregates (sand, gravel, stone), water and cement. These ingredients bond during a process called hydration. Another positive is the fact that concrete is eminently accessible. Concrete independently has great compression strength, however it is weak in tensile strength. This considered, steel bars was included in order to increase the tensile strength of the elements.

There are several parameters that affects the end product of the concrete. The water/cement ratio is a crucial factor in concrete mixture. The reason for this is the correlation between water and cement. More cement (or less water) equals a higher strength. However, there has to be some water in a concrete mixture. Combined, the water and cement are the glue in fresh concrete and are also known as cement-paste. Through the chemical reaction known as hydration, the cement-paste hardens. The aggregates in the concrete, the water, and the cement, creates a bond and gains strength. Because of this relationship between the water and cement, the amount of each substance in the mixture is essential to make the appropriate concrete. Too much water will give a lower strength. Not enough water will give a mixture with lower workability.

Another important ingredient in the concrete are the aggregates. Sand, gravel and crushed stones are the most common aggregates to use. Sand, gravel and crushed stones usually have different sizes. Aggregate grading is the distribution measure of the aggregate particle sizes in the mixture. A well graded aggregate mixture has a large distribution of sizes, while a poorly graded aggregate will have aggregate particles of only some sizes and be poorly distributed. In order to reduce the shrinkage of the concrete, a well graded mixture of aggregates is preferred. In a concrete mix, it is the cement paste that causes the shrinking. Therefore, the cement paste had to be limited

to the minimal. A well graded aggregate mixture will also improve the workability of the concrete. In most cases the aggregates accounts for around 60 - 75 percent of the concrete volume. The selection of aggregates are therefore important.

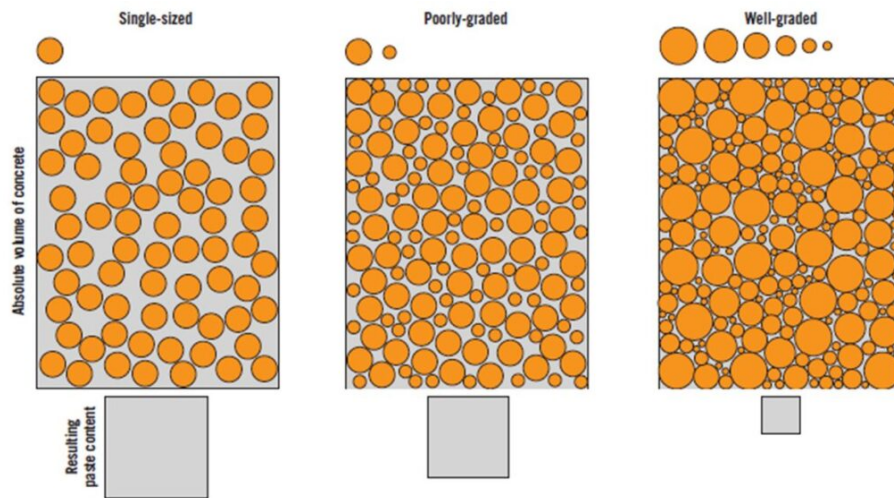


Figure 3.8: Grading of aggregates in concrete: Single sized, poorly sized and well-graded

Superplasticizers (and regular plasticizers) are used as high range water reducers. With the use of superplasticizers the water usage decreases by a significant figure. Environmentally, this could make a large difference. Superplasticizers are also used to improve the workability of the concrete. Because of the large span of different usage of concrete, plasticizers and superplasticizers are essential. Adding water to increase the workability will affect the strength in the end product.

Fly ash is also an ingredient often used when mixing concrete. Fly ash is a byproduct produced when burning pulverized coal in an electric generation power plant and it can be used for a number of reasons. In short, the fly ash decreases water demand, improves workability and reduces the heat of hydration in the fresh concrete. In the hardened concrete, the fly ash increases the ultimate strength, reduces the permeability (the ability of the given concrete to let liquids or gases to flow through) and the durability is increased.

The process of curing is used to keep the desired moisture and temperature in the concrete [11] and is an important step in order to gain the necessary concrete strength. The durability of the concrete is also dependent on the curing and it starts immediately after the fresh concrete is cast. Mixing ratio is given below:

Materials	Quantity kg/m^3
Gravel 8-16mm	672.184
Gravel 8mm sand	896.246
Gravel 2mm sand	302.143
Silica	11.274
Fly Ash	20.498
Standard cement FA	309.860
Cold water	152.272
Air	0.342
Pump oil	0.683
Dynamon SX-23	2.221
Total	2367.723

Table 4: Mixing ratio

3.5.1 Specimens for testing

As mentioned, there were six specimens with 300x300x2000mm dimensions. For each of these specimen, 180 litres of concrete were used. Due to the large volume needed, we ordered the concrete from Sola Betong AS. The recipe of the concrete can be found in appendix A.1.

3.5.2 Cubes and cylinders for testing

In addition to the six larger specimens, there was prepared 3 cubes with dimensions 100x100x100mm, and 12 cylinders with a height of 300mm and a diameter of 150mm. There was also cast 1 specimen for a fracture energy test. The specimens were put in water during the curing process in order to maintain humidity.



Figure 3.9: Cast concrete for testing

3.5.3 Volume calculations

The total volume that were utilized for the specimens used in this research, is shown in the table below. The table shows how much concrete was needed from the concrete truck ordered from Sola Betong AS. 180 litres of concrete in each specimen, and polyethylene to keep the humidity in.

Form	Volume
6 Specimens	1.08 m^3
12 cylinders	0.063617 m^3
3 cubes	0.010125 m^3
Fracture energy specimen	0.003285 m^3
Total volume	1.157027 m^3

Table 5: Concrete order

3.8

Approximately 1500 litres of concrete were needed in the casting process.

3.6 Test set up at IKM

As mentioned, the main test for this project was completed at the IKM Laboratory at Tananger, Norway. The specimens were shipped from the university to the laboratory. At IKM, the specimens would be tested by a "force-controlled" bench and recorded by the DIC instrument to measure the strain. The tests could only be done with one specimen at a time, and because there was only one pair of load connections for each concrete cover thickness, the tests needed to be completed in the right order to preserve the load connections. Shown in figure 3.10 and figure 3.11 is the idea behind the test set-up. The load will be applied from the load connections. First the 35mm cover thickness, then 60mm and lastly the 85mm. Before each test, the DIC instrument had to be calibrated for the specimen. In order to get the right calibration, the specimens were spray painted white, with black dots. During the tests, everyone had to be clear of the danger zone because of the great amount of load on the beams. As seen in the image below, the beams were attached on each side. After each test the specimens were lifted away from the bench and the load connection had to be taken off and applied to the next specimen.



Figure 3.10: Test set up at IKM

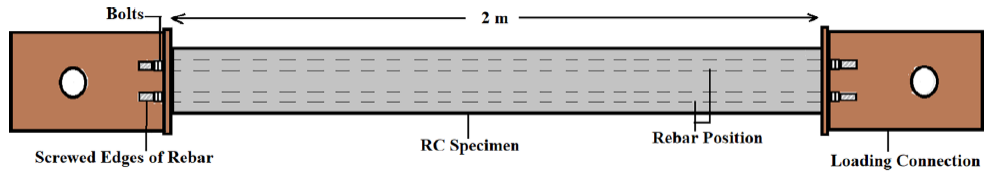


Figure 3.11: Illustration from Naotunna et AL [1]

4 Results of the Experiment

4.1 Compressive test

To test the compression, a Toni Technik test was used on three cubes and three cylinders. The cube or cylinder is placed in the middle of the machine and a continuously increasing pressure is applied to the specimen until failure. In total, three specimens were tested, and the average stress of all three determines the strength of the concrete.

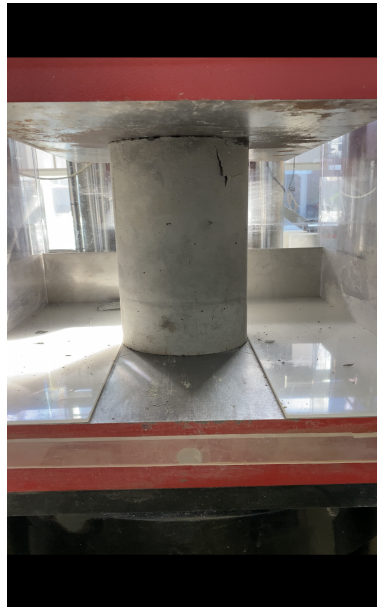


Figure 4.1: Compression Test

Results of the test

The compression test was conducted on March 17th and the concrete was cast January 28th, so the tests were conducted later than usual. When calculating the expected compressive strength the air content of the concrete must be considered. The air content of the concrete was not measured before testing, which means the air content must relate to the measure from the matrix of the concrete. From the matrix, the air content is measured to be 2% . Then the expected compressive strength is:

$$f_c = 35N/mm^2 * 98 = 34.3N/mm^2\%$$

Specimen	Maximum force F_m [kN]	Stress σ_m [N/mm^2]
Cylinder 1	695.58	39.36
Cylinder 2	726.18	41.09
Cylinder 3	749.17	42.39
Average stress		40.95

Table 6: Compression test

3.8

From the results it is noticeable that the compressive strength of the concrete is higher than the expected strength. From the national standard the average stress is equal to the compressive strength (f_c). There is an increase of approximately 6 MPa from the test, to the standard. More specimens for testing would have given a more accurate result.

4.2 Young's modulus test

Young's modulus, or E-modulus, measures the material resistance to elastic elongation. The strain and stress is measured when the material undergoes elastic deformation through compressing and extension, and when the load is removed it will go back to it's original shape. The E-modulus is calculated with the expression below:

$$E = \frac{\sigma}{\epsilon}$$

When conducting the E-modulus test, method A from the national standard was used. For calculating the E-modulus there is a device clipped on to the specimen and then the specimen is

placed axially in the center of the press. σ_b and σ_p are the top and bottom stress limits and these have to be calculated in order to do the test. The calculations are given below:

$$\sigma_a = \frac{f_c}{3}$$

$$0.10 * f_c \leq \sigma_b \leq 0.15 * f_c$$

$$0.5MPa \leq \sigma_p \leq \sigma_b$$

The test starts off with three preloading cycles to ensure the positioning of the specimen and the stability of the wires. After the preloading cycles, three loading cycles with higher stress will be carried out to obtain the initial and stabilized modulus of elasticity. The initial modulus of elasticity will be calculated during the start of the test, and the stabilized modulus of elasticity will be calculated during the final part of the test. The calculations are done with the equations below:

$$E_{C,0} = \frac{\Delta\sigma}{\Delta\epsilon_0} = \frac{\sigma_a^m - \sigma_b^m}{\epsilon_{a,1} - \epsilon_{b,0}}$$

$$E_{C,S} = \frac{\Delta\sigma}{\Delta\epsilon_S} = \frac{\sigma_a^m - \sigma_b^m}{\epsilon_{a,3} - \epsilon_{b,2}}$$

$E_{C,0}$ - initial modulus of elasticity in GPa (kN/mm^2)

$E_{C,S}$ - stabilized modulus of elasticity in GPa (kN/mm^2)

σ_a^m - upper measured stress in MPa (N/mm^2)

σ_b^m - lower measured stress in MPa (N/mm^2)

$\epsilon_{a,n}$ - upper strain on loading cycle n in

$\epsilon_{b,n}$ - lower strain on loading cycle n in

Results of the test

In order to get more accurate and better results, the concrete cylinders had to be cut at the top and bottom. Due to this issue, the available specimens were few. The Young's modulus test was performed on two specimens, and the table below shows the results from the test.

Specimen	$E_{c,0}$ [N/mm^2]	$E_{c,s}$ [N/mm^2]
Specimen 1	8 332	11 677
Specimen 2	9 514	12 478

Table 7: Young's modulus

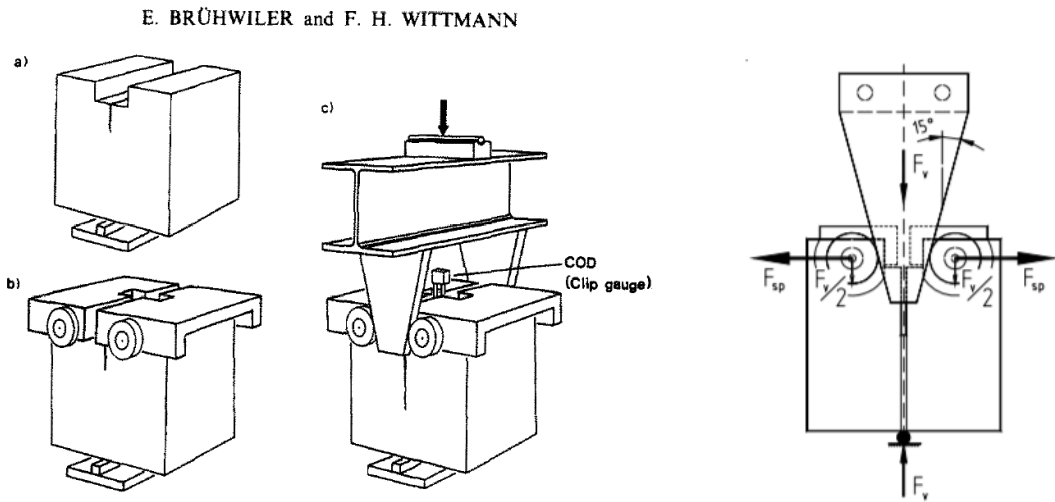
3.8

From the table, it is noticeable that the results from the test is not the desired results. Since the test could only be conducted on two specimens, it is hard to determine if there was a test failure, or a failure of the concrete. The B35 strength class requires a stabilized modulus of elasticity of $34\,000\ N/mm^2$ and the largest measured value from this test was $12\,478\ N/mm^2$, not nearly enough to qualify for the B35 class.

Due to the test failure, the required stabilized modulus of elasticity of $34\,000\ N/mm^2$ will be used for the calculations later.

4.3 Fracture energy - Wedge splitting test

To measure the fracture mechanics of the concrete, the Wedge Splitting Test (WST) method from the Swiss Federal Institute of Technology [2] was used. This is a result of the WST not being a part of the Norwegian National Standard. The objective of the Wedge Splitting Test (WST) is to perform solid fracture mechanic tests on concrete. WST measures the amount of energy required for the concrete to split/come apart. Fracture energy does not depend on size, because it is a material property. The set-up of the test is shown in figure below.



(1) Principle of the wedge splitting test: (a) test specimen on a linear support; (b) placing of two loading devices with rollers; and (c) the wedges are pressed between rollers in order to split the specimen into two halves.

(2) Principle of applying the splitting load F_s .

Figure 4.2: Setup for wedge splitting test [2]

When casting the cubic specimens for the WST we had a premade formwork. The hardened specimen had a cast groove in the upper part as shown in the figure 4.3. The indent/notch in the specimen is to ensure a stable crack initiation when testing. When hardened for at least 28 days, the specimen is ready for the WST. The specimen is then placed on a top of a loading cell. We used polystyrene in order to stabilize the specimen on top of the loading cell. On both sides of the groove, a steel loading device with roller bearings are placed. When applying the vertical force (F_v) with the wedging device, the Crack Opening Displacement (DOC) is measured with the clip gauge, which is fastened in the center of the notch. When applying the F_v the fracture section is

principally subjected to bending moment. The vertical force from the wedge is translated into a horizontal force acting on the rollers. The horizontal force is the splitting force F_s which correlates with the bending moment. The idea is shown above in figure 4.2.2. From the relationship between the angle of the wedge and the vertical force, the splitting force can be calculated as shown in the equation below.

$$F_s = \frac{F_v}{2 \cdot \tan \alpha}$$

We can acquire the energy needed in order to split the specimen in half from calculating the area underneath the F_s -COD curve. Taking this energy and dividing it by the projected fracture area, the total fracture energy can be found. The projected area equals the specimen depth (d) multiplied with the height of the specimen (h) minus the groove. The results are given in table 8. The Force-COD curve for the WST are shown in figure 4.3.

	Maximum vertical force F_v [kN]	Maximum splitting force F_s [kN]	Total fracture energy G_F [kJ/m ²]
Specimen 1	3.90 kN	7.48 kN	

Table 8: WST test results

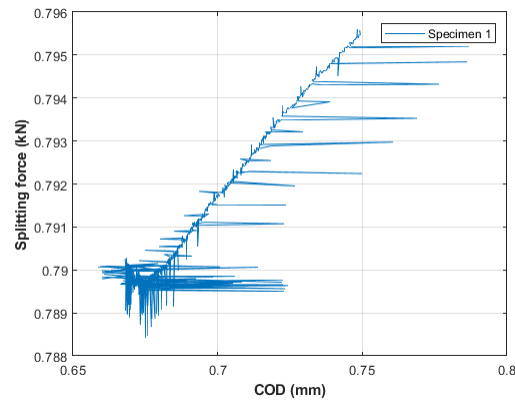
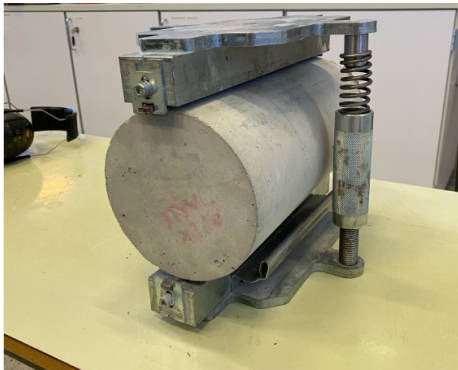


Figure 4.3: F_s - COD graph

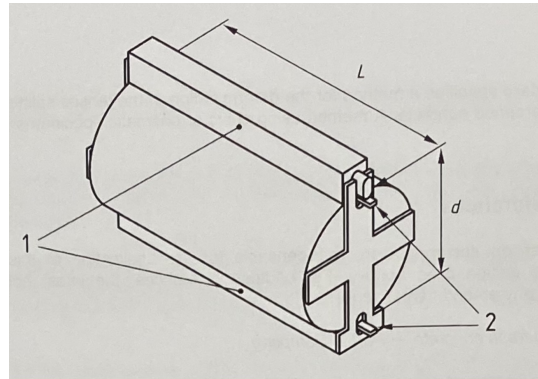
The figure implies that there has been errors during the tests. In combination with the fact that only one specimen was tested, the results were disregarded.

4.4 Splitting tensile test

Tensile strength in the concrete specimen greatly affects the cracking of the concrete. Cracks may occur when the concrete is subjected to more tension than the tensile strength of the concrete. The splitting tensile test is used to determine the tensile strength of the concrete. The test is executed as explained in NS-EN 12390-6:2009 and will be performed in the same machine as the compressive test. From the moulds, cylindrical specimen of concrete are made. The cylinder is positioned vertically inside a steel frame and placed inside the Toni-technik machine for compressive strength as shown in the picture.



(1) Set up of the cylinder into the steel frame/jig



(2) Dimensions for the tensile splitting test

Figure 4.4: Splitting tensile test

A continuously increasing load is applied on the specimen until it cleaves/splits in half. Assuming the concrete has an elastic behaviour, the tensile strength can be calculated from the equation 1 below.

$$f_{ct,sp} = \frac{2 * F}{\pi * d * L} \quad (1)$$

$f_{ct,sp}$ - Splitting tensile strength, measured in Megapascal (MPa) - $\frac{N}{mm^2}$

F - Maximum applied load in Newtons (N).

d - cross-sectional diameter of the specimen, measured in millimeters (mm)

L - length of the specimens contact surface, measured in millimeters (mm)

In normal strength concrete, the tensile strength averages around 10% of the compressive strength. The specimens were made from B35 concrete. The compressive strength of B35 class concrete should be around 35 MPa. In theory the tensile strength of the specimens should be 3.5 MPa.

Specimen number	Maximum force applied f_{cm} [kN]	Tensile strength $f_{ct,sp}$ [N/mm^2]
1	238.95	3.38
2	190.07	2.69
Average	214.51	3.035

Table 9: Splitting tensile test results

From the results it is noticeable that the average is lower than the theoretical approach. Two test specimens might not suffice. Similar to the Young's modulus test, it is hard to determine whether it is a failure of the concrete or if it is a test failure, since only two specimens was used for testing. The results show 86.7% of the theoretical tensile strength. Comparing with a splitting tensile test executed a couple days earlier from the same concrete batch.

Specimen number	Maximum force applied f_{cm} [kN]	Tensile strength $f_{ct,sp}$ [N/mm^2]
1	234.15	3.31
2	239.81	3.39
Average	236.98	3.35

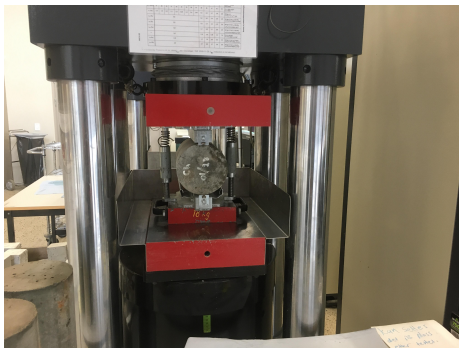
Table 10: Splitting tensile test results from earlier test

Comparing the results, the tensile strength of the concrete specimens are acceptable.

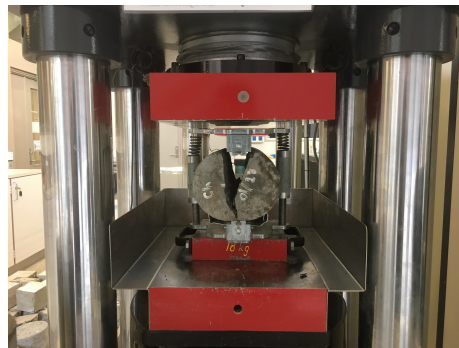
According to EC2 section 3.3: An approximate value f_{ct} should be taken from the determined $f_{ct,sp}$ as:

$$f_{ct} = 0.9f_{ct,sp} \quad (2)$$

According to the equation from EC2, the tensile strength of the test specimens are approximately 2.73 MPa. If the two tests and the four results are combined, the tensile strength are approximately 2.87.



(1) Splitting tensile before



(2) Splitting tensile after

Figure 4.5: Splitting tensile test

4.5 IKM test - Axial tensile strength. Crack spacing

The test was conducted at the IKM laboratory at Tananger the 9th of March, 2021. As explained above, the critical point in the steel design were the threaded sections of the reinforcement. Calculated, the breaking point would be at approximately 90 tonnes of loading. For the first beams, the load was increased in 10KN each step, and the loading was not increased past 80KN. For the last specimens, the breaking point of the steel design were tested as well. The loading was increased, until the threaded section of the reinforcement reached it's ultimate state. The load at the given time is shown in the appendix for each individual specimen. From 70KN, the loading was kept at the same amount for several minutes, before it was increased to the next step in the process. In table 11 below, the maximum applied load is shown. Comparing the results below, with the theoretical design resistance from 3 it is apparent that some of the connections surpass the design resistance before reaching the breaking point. This is due to the safety factors used while calculating according to the NS-EN 1993: 1.8.

Beam number	Concrete cover	Maximum applied force in tonnes (kN)
1	85 mm	90.49 tonnes (887.4 kN)
2	35 mm	80.29 tonnes (787.4 kN)
3	85 mm	93.95 tonnes (921.3 kN)
4	35 mm	80.46 tonnes (789.0 kN)
5	60 mm	82.32 tonnes (807.3 kN)
6	60 mm	90.12 tonnes (883.8 kN)

Table 11: Maximum applied force on beams at IKM

The force was measured in tonnes at IKM in Tananger. As shown in appendix B.4-B.9, the results were given in tonnes. One tonne equals to 9.80665 Kilo Newtons. As shown in the table 11 above, force in Kilo Newtons as well. The steel design, and other calculations were done in Kilo Newtons. As shown in the figure B.6 and figure B.8 the loading stops abruptly. This is the breaking point of the threaded section of the reinforcement. As shown in the image below, the reinforcement could not withstand the loading.

Due to the failure of the DIC, the analysis could not give us the number of the strain or the crack width. The resolution of the pictures only showed the cracks at the end of the test, and therefore they can not be used to see when the cracks started to occur.



Figure 4.6: Threaded section after surpassing maximum design resistance

5 Comparisons between experimental findings and literature

5.1 Experimental findings

After the experiment was conducted at the IKM Tangerang, the cracks were marked and measured to calculate the crack spacing of the specimens. From literature, we know that the crack spacing is shorter with smaller concrete cover distance. When measuring the crack spacing manually, it may be some deviance of the measuring accuracy. The design of the load connections and the reinforcement was also tested during the main test at the IKM. From the results shown in section 5.1.1, we see that the load connections could withstand the force it was designed to handle. On the other hand, there were two sets of reinforcement where one of the sets were not as capable of withstanding the force as the other set. The source of this issue was most likely that the reinforcement bars were manually threaded at the machine lab at UiS. The main test at the IKM was monitored by a Digital Image Correlation (DIC) with the purpose of analysing the strain and crack width during the test. As mentioned, the DIC failed due to poor calibration. The experimental findings from the main test, without the results from the DIC, were mostly surrounding the design of the load connections, reinforcement and the crack spacing.

5.1.1 IKM Test

The "force-controlled" bench at the IKM Laboratory in Tangerang was able to adjust the force put onto the specimen in steps with an increase of 100kN. The load connections were designed to withstand a force of between approximately 800kN and 900kN. From the results, it is apparent that the load connections were capable of withstanding the force they were designed to carry. When testing the specimens, it was experienced that the "force-controlled" bench was not able to carry the beams without an angle. This issue meant that there would be some deviation in the results and could be causing the specimens to fail where they were not supposed to. The angle of the specimens were possibly one of the sources to the issue with the DIC, alongside the calibration and change of lighting in the laboratory.

5.1.2 Crack Spacing

With different concrete cover, it is important to analyse the crack spacing data. When measuring the crack spacing, it was noticeable that the cover thickness impacted the crack spacing. As seen in the results, the amount of cracks increased, whereas the spacing decreased, with smaller cover thickness. When searching for cracks using an optical microscope the reliability of the analysis will be reduced. This issue was corresponding for the studies of Rimkus et al.(2019). [6] The crack spacing of one face of the beams with 35mm, 60mm and 85mm is shown in figure 5.1, 5.2 and 5.3. The other pictures are given in the appendix D.1-D.24.

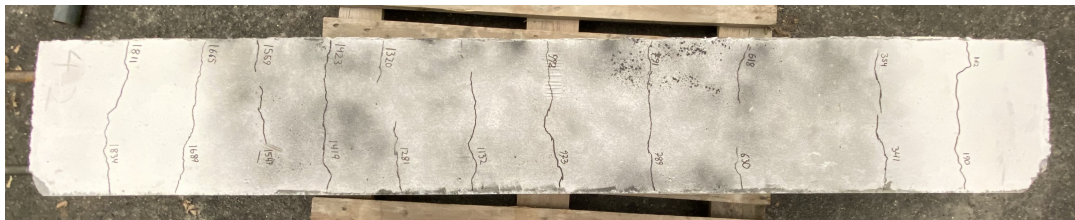


Figure 5.1: 35 mm cover



Figure 5.2: 60 mm cover



Figure 5.3: 85 mm cover

Concrete cover thickness	Mean value	Standard deviation
35 mm	177.78 mm	55.5
60 mm	200 mm	66.2
85 mm	212.2 mm	68.6

Table 12: Mean values and Standard deviation of crack spacing

5.2 Theoretical assumptions from literature

The EC2 and the MC2010 uses a semi-analytical crack width calculation model where they predict the crack width by multiplying the mean stress with the crack spacing. When calculating the crack spacing, or the transfer length, from the Eurocode 2 and the Model Code 2010 it is important to keep in mind that the formulations from the two standards are considered conservative by researchers. As previously mentioned, the current standards focus on the maximum values for the crack width, and this may be an issue in the design stage. From earlier studies, we can assume that the pattern of cracks will look similar when conducting an experiment with four reinforcement bars and shorter concrete cover thickness. The studies of Rimkus shows that the calculations from the EC2 and the MC2010 predicts that the maximum crack spacing is dependent on the $\frac{\phi}{p}$ while the test results were practically independent from the reinforcement characteristics. However, this experiment was conducted using only one bar diameter, while the results from the studies of Rimkus [6] discusses the importance of the right concrete cover thickness.

When calculating the crack width and the crack spacing with the formulations from the EC2 and the MC2010, it was considered a "short-term loading condition" in the "stabilized cracking stage". The whole cross section area of the specimen was assumed for the "effective tensile area of the concrete". This assumption was made because of the fact that most cracks propagate from reinforcement bars to the surface of the specimen.

5.2.1 Crack spacing

Calculations from Eurocode:

From testing in laboratory:

From the Eurocode 2 it is given that the crack width and crack spacing are calculated from the equation below:

$$s_{r,max} = k_3 c + \frac{k_1 k_2 k_4 \phi}{p p, eff}$$

From the Eurocode 2:

$$k_1 = 0.8 \quad k_2 = 1.0 \quad k_3 = 3.4 \quad k_4 = 0.425$$

Other parameters:

$$\phi = 32mm$$

$$c = 35mm/60mm/85mm$$

$$A_{s,bar} = \frac{(\phi^2 * \pi)}{4} = 804.2477mm^2$$

$$A_{s,tot} = A_{s,bar} * 4 = 3216.990mm^2$$

$$A_{cef} = 300mm * 300mm = 90000mm$$

$$P_{p,eff} = \frac{A_s}{A_{cef}} = \frac{3216.990mm}{90000mm} = 0.0357$$

Calculations of the maximum crack spacing:

35 mm concrete cover:

$$s_{r,max} = k_3c + \frac{k_1k_2k_4\phi}{pp,eff} = 3.4 * 35mm + \frac{0.8*1.0*0.425*32mm}{0.0357} = 423.76mm$$

60 mm concrete cover:

$$s_{r,max} = k_3c + \frac{k_1k_2k_4\phi}{pp,eff} = 3.4 * 60mm + \frac{0.8*1.0*0.425*32mm}{0.0357} = 508.76mm$$

85mm concrete cover:

$$s_{r,max} = k_3c + \frac{k_1k_2k_4\phi}{pp,eff} = 3.4 * 85mm + \frac{0.8*1.0*0.425*32mm}{0.0357} = 593.76mm$$

Calculations of the crack width:

From testing:

$$f_{ct} = 2.87N/mm^2$$

$$E_c = 34000N/mm^2$$

Other parameters:

$$E_s = 200000N/mm^2$$

$$\alpha_e = \frac{E_s}{E_c} = 5.8824$$

Calculations:

From Table 9 the average load for each cover thickness is:

35mm cover: 788.2 kN

$$\sigma_{s,35mm} = 245MPa$$

60mm cover: 845.55 kN

$$\sigma_{s,60mm} = 262.8MPa$$

85mm cover: 904.35 kN

$$\sigma_{s,85mm} = 281.1MPa$$

Crack width:

35 mm cover:

$$\epsilon_{cr} = \epsilon_{sm} - \epsilon_{cm} = \frac{\sigma_{s,35mm} - k_t \frac{f_{ct,eff}}{P_{p,eff}} (1 + \alpha_e P_{p,eff})}{E_s} = 0.000836$$

$$\epsilon_{min} = 0.6 * \frac{\sigma_{s,35mm}}{E_s} = 0.000735$$

$$\epsilon_{cr} > \epsilon_{min}$$

Use ϵ_{cr} :

$$wk = s_{r,max}(\epsilon_{cr}) = 0.3543mm$$

60 mm cover:

$$\epsilon_{cr} = \epsilon_{sm} - \epsilon_{cm} = \frac{\sigma_{s,60mm} - k_t \frac{f_{ct,eff}}{P_{p,eff}} (1 + \alpha_e P_{p,eff})}{E_s} = 0.0009224$$

$$\epsilon_{min} = 0.6 * \frac{\sigma_{s,60mm}}{E_s} = 0.0007884$$

$$\epsilon_{cr} > \epsilon_{min}$$

Use ϵ_{cr} :

$$wk = s_{r,max}(\epsilon_{cr}) = 0.4693mm$$

85 mm cover:

$$\epsilon_{cr} = \epsilon_{sm} - \epsilon_{cm} = \frac{\sigma_{s,85mm} - k_t \frac{f_{ct,eff}}{P_{p,eff}} (1 + \alpha_e P_{p,eff})}{E_s} = 0.00101$$

$$\epsilon_{min} = 0.6 * \frac{\sigma_{s,85mm}}{E_s} = 0.0008433$$

$$\epsilon_{cr} > \epsilon_{min}$$

Use ϵ_{cr} :

$$wk = s_{r,max}(\epsilon_{cr}) = 0.5997mm$$

Calculations from Model Code 2010:

$$l_{s,max} = k * c + \frac{1}{4} * \frac{f_{ctm}}{\tau_{bms}} * \frac{\phi_s}{p_{s,ef}}$$

$$k = 1$$

c= concrete cover thickness - 35mm/60mm/85mm

$$f_{ctm} = 3.035N/mm^2$$

$$A_{s,bar} = \frac{(\phi^2 * \pi)}{4} = 804.2477mm^2$$

$$A_{s,tot} = A_{s,bar} * 4 = 3216.990mm^2$$

$$A_{cef} = 300mm * 300mm = 90000mm$$

$$P_{p,eff} = \frac{A_s}{A_{cef}} = \frac{3216.990mm}{90000mm} = 0.0357$$

Short-term, instantenous loading:

$$\tau_{bms} = 1.8 * f_{ctm}$$

35 mm concrete cover:

$$l_{s,max} = k * c + \frac{1}{4} * \frac{f_{ctm}}{\tau_{bms}} * \frac{\phi_s}{p_{s,ef}} = 1 * 35mm + \frac{1}{4} * \frac{3.035N/mm^2}{1.8*3.035N/mm^2} * \frac{32mm}{0.0357} = 159.5mm$$

60 mm concrete cover:

$$l_{s,max} = k * c + \frac{1}{4} * \frac{f_{ctm}}{\tau_{bms}} * \frac{\phi_s}{p_{s,ef}} = 1 * 60mm + \frac{1}{4} * \frac{3.035N/mm^2}{1.8*3.035N/mm^2} * \frac{32mm}{0.0357} = 184.494mm$$

85 mm concrete cover:

$$l_{s,max} = k * c + \frac{1}{4} * \frac{f_{ctm}}{\tau_{bms}} * \frac{\phi_s}{p_{s,ef}} = 1 * 85mm + \frac{1}{4} * \frac{3.035N/mm^2}{1.8*3.035N/mm^2} * \frac{32mm}{0.0357} = 209.4942mm$$

Calculations of crack width:

Maximum steel stress at crack formation stage:

$$\sigma_{sr} = \frac{f_{ct}}{p_{p,eff}} * (1 + \alpha_e * p_{p,eff}) = 97.275MPa$$

Mean strain difference of steel and concrete:

35mm cover:

$$\epsilon_m = \frac{\sigma_s - \beta * \sigma_{sT}}{E_s} = 0.0009331$$

60mm cover:

$$\epsilon_m = \frac{\sigma_s - \beta * \sigma_{sT}}{E_s} = 0.001022$$

85mm cover:

$$\epsilon_m = \frac{\sigma_s - \beta * \sigma_{sT}}{E_s} = 0.001114$$

Crack width:

35mm cover:

$$W_d = 2 * l_{s,max} * \epsilon_m = 0.2977mm$$

60mm cover:

$$W_d = 2 * l_{s,max} * \epsilon_m = 0.3771mm$$

85mm cover:

$$W_d = 2 * l_{s,max} * \epsilon_m = 0.4668mm$$

5.2.2 Differences in cover for reinforcement

From the calculations above, it is clear that from the EC2 and MC2010 the cover for reinforcement is one of the main parameters for the crack spacing and the transfer length. From the results of the experiment for this thesis, it is noticeable that the concrete cover is a governing parameter for the crack spacing and the crack width. Some researchers want to see a bigger effect of the bar diameter, although Rimkus [6] states that the difference in bar diameter did not largely affect the result of the crack spacing. Keeping this in mind, it is clear that difference in the cover for reinforcement is very controlling when measuring the spacing.

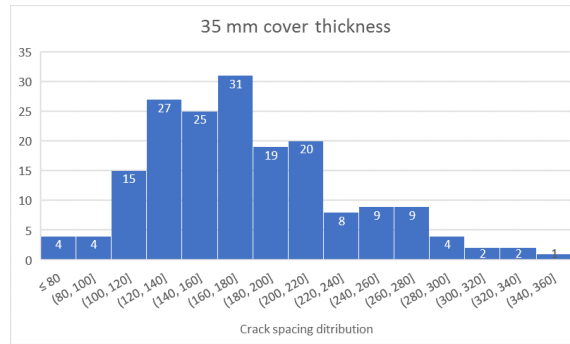
As mentioned, the covers of 35mm, 60mm and 85mm were use for this experiment. The difference in cover reflects the results, where the specimens with the smallest cover generated more cracks and a smaller crack spacing.

6 Discussion

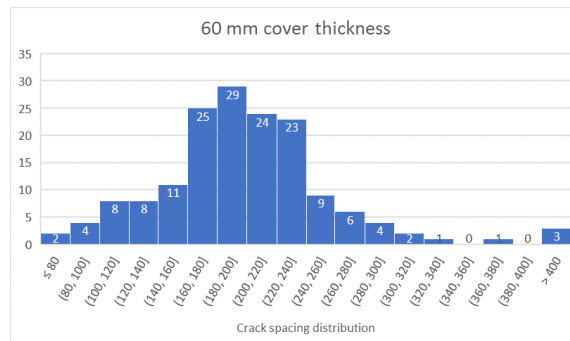
6.1 Experimental investigation of crack spacing

To verify the experimental findings, it is important to compare the results of this thesis to similar experiments. The maximum to mean crack spacing values vary from 1.2 to 1.9 from the results. This ratio is supposed to vary from 1.2 to 1.7, but due to limitations when measuring, the ratio is higher than expected. When excluding the results that most likely is high due to poor measuring, the value of maximum to average spacing vary from 1.2 to 1.7.

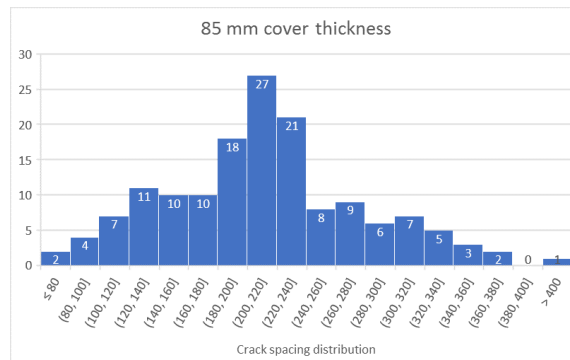
Figure 6.1 shows the crack distribution for each of the three cover thicknesses. From the histogram, it is noticeable that the majority of the spacing values for the 35mm cover vary from 100mm to 220 mm. As seen from Table 12, the mean value for the 35 mm cover is 177.78mm. When comparing this to the calculations from the EC2 and the MC2010, the majority of the values are half the maximum crack spacing. This comparison is corresponding for the 60mm and 85mm cover, where the mean value for 60mm is 200mm, and 212.2mm for the 85mm. From the histograms, it is clear that the smaller cover distances produces a more distributed crack spacing data. Comparing the 85mm to the 35mm, it is clear that the 85mm is peaking with values from 180mm to 240mm, while the 35mm is more evenly distributed in the area from 100mm to 220mm. In total, it was possible to measure 151 cracks for the 85mm cover, 160 cracks for the 60mm cover and 180 cracks for the 35mm cover.



(1) Histogram 35 mm



(2) Histogram 60 mm



(3) Histogram 85 mm

Figure 6.1: Histogram of crack spacing distribution

6.2 Formulations from the Eurocode 2 and Model Code 2010

As previously mentioned, the calculations from both the Eurocode 2 and the Model Code 2010 are considered conservative. Researchers, like Tan et al.(2018) [7], analysed the calculations models

for the EC2 and the MC2010, where both models are very much alike. From this research, it is suggested that the calculations of the crack spacing, or the transfer length, is in conflict with the basic principles of solid mechanics. These models are according to Tan et al.(2018) [7], merging the bond-slip theory and the no-slip theory into one formulation. These two theories are based on opposite assumptions and therefore the models can be considered inconsistent.

This experiment focus on the importance of the concrete cover thickness, and experimental studies supports the theory of the concrete cover being the main parameter when calculating the crack spacing. Researchers have noticed the limited influence of the bar diameter. The bar diameter has a beneficial effect for reducing the transfer length, although it is not heavily emphasized in the models from EC2 and MC2. While Tan wishes a greater emphasis of the reinforcement bar characteristics, other studies shows the lack of influence from the reinforcement. From the studies of Rimkus et al.(2019) [6] it is implied that the calculations from the EC2 and the MC2010 with different bar diameters have a much greater impact than the experimental investigation would suggest.

7 Conclusion

The objective for this thesis was to conduct an experimental investigation of crack spacing to observe the behaviour of cracks in reinforced concrete structures with different cover thickness, and verify the results with similar experiments. The earlier studies on this subject is substantial, and therefore this experiment was conducted focusing on the crack spacing. The aim of the experiment was to compare results of the crack spacing with different concrete cover thicknesses when applying axial tensile load. The next aim for the project was to compare these results to the calculations made from the Eurocode 2 and the Model Code 2010. When examining the crack spacing from the specimens, it is clear that the cover thickness is an important parameter. From the results we see that with a reduction in cover thickness, the crack spacing reduces and the amount of cracks increase. This was an assumption made from literature and it has been verified by the results from our experiment. Furthermore, the formulations from the Eurocode 2 and Model Code 2010 have, from literature, been considered conservative. From the earlier calculations in the thesis, it is clear that the maximum crack spacing results is not the equivalent to the results from the calculations. Due to the failure of the DIC we were unable to compare the crack width and strain from the experiment to the results from the Eurocode 2 and the Model Code 2010.

7.1 Recommendation for further research

Overall, the experiment conducted for this thesis was a success, but after completing this research it would be interesting to observe other similar experiments. The recommendation is to conduct an experiment with different concrete cover thickness in reinforced concrete structures with different sizes of the bar diameter. The objective with such an experiment would be to observe the cracking behaviour with different bar diameter and compare the results to the calculations from the Eurocode 2 and the Model Code 2010. As previously explained, the researchers Tan et al.(2018) [7] and Rimkus et al.(2019) [6] have two opposite views of the effect of the bar diameter, therefore it would be interesting to see the effect of the bar diameter while keeping the same and using different concrete cover thickness.

References

- [1] C. N. Naotunna, S. S. MK Samarakoon, and K. T. Fosså, “Experimental and theoretical behavior of crack spacing of specimens subjected to axial tension and bending,” *Structural Concrete*, 2020.
- [2] E. Brühwiler and F. Wittmann, “The wedge splitting test, a new method of performing stable fracture mechanics tests,” *Engineering fracture mechanics*, vol. 35, no. 1-3, pp. 117–125, 1990.
- [3] E. . Sohn, “Model code for concrete structures,” The International Federation for Structural Concrete, Standard, 2010.
- [4] F. Barre, P. Bisch, D. Chauvel, J. Cortade, J.-F. Coste, J.-P. Dubois, S. Erlicher, E. Gallitre, P. Labbé, J. Mazars *et al.*, *Control of cracking in reinforced concrete structures: Research project CEOS. fr.* John Wiley & Sons, 2016.
- [5] “Eurocode 2: Design of concrete structures - part 1-1: General rules and rules for buildings,” European Standard, Standard, dec 2004.
- [6] A. Rimkus and V. Gribniak, “Experimental investigation of cracking and deformations of concrete ties reinforced with multiple bars,” *Construction and Building Materials*, vol. 148, pp. 49–61, 2017. [Online]. Available: <https://www.sciencedirect.com/science/article/pii/S0950061817309212>
- [7] R. Tan, K. Eileraas, O. Opkvitne, G. Žirgulis, M. A. Hendriks, M. Geiker, D.-E. Brekke, and T. Kanstad, “Experimental and theoretical investigation of crack width calculation methods for rc ties,” *Structural Concrete*, vol. 19, no. 5, pp. 1436–1447, 2018.
- [8] “Eurocode 3: Design of steel structures,” Norsk Standard, Standard, oct 2009.
- [9] J. Kerns, “What’s the difference between bearing, shear, and tear-out stress?” jul 2016. [Online]. Available: <https://www.machinedesign.com/fasteners/what-s-difference-between-bearing-shear-and-tear-out-stress>
- [10] D. Sonck, N. Boissonnade, and R. Van Impe, “Instabilities of cellular members loaded in bending or compression,” in *Proceedings of the Annual Stability Conference Structural Research Council*, 2012, p. 19.
- [11] S. H. Kosmatka, B. Kerkhoff, W. C. Panarese *et al.*, *Design and control of concrete mixtures.* Portland Cement Association Skokie, IL, 2002, vol. 5420.

A Concrete Matrix

A.1 Sola betong matrix

Tel.: +47 51 64 49 49
W...: @...: post@sola-betong.no

BR_ASL

Resept opplysninger

Resept : 251 ~ B35 M45 SKB dmax 16 std FA SF2
 Oprettet av : Rune Dato : 18-10-2016 13:02:41
 Redigert av : proces Dato : 12-11-2019 09:53:51
 Resepttype : Fast verdi Status : Aktiv
 Konsistenstype : Synkubredningsmål
 Varepris navn : Varepris : B23516003000
 Familie : B Familie navn : standard fa u/luft
 Tilslagspec. : 11 SKB ~ SKB 16
 Bindemiddel spec. : 71 ~ Std Fa 90 10 Flyveaske 3,3% SILICA
 Vannspec. : 01 ~ Kaldt Vann
 Kjemispec. : 31 B35 SKB ~ SX 23 1,0 %+ luft 0,1%

Standard : NS206

VC spec.nr. : V/C-Forhold : 0,447
 Bestandighetsklasse : M45 Ameringstål : Ingen valgt
 Klorklasse : Cl 0,10 Kontrollklasse : Ingen valgt
 Modenhetsminutter : Klassifikasjon : Designet
 Fasthetsklasse : B35 Manuel børverdi : 60
 M³ siden siste prøve(fam.): 91,15 M³ siden siste prøve : 19,00
 Rct.prv.hyp. i periode : 30,76
 Eksponeringsklasse : X0, XC1, XC2, XC3, XC4, XF1, XD1, XS1, XA1, XA2, XA4

Stamopplysninger

Min. sement innhold : Nei
 Min. sement innhold : Max :
 Min. filler innhold : Max :
 Synkutbredelsesinterval : 500 - 700 Betongtype :
 Bruk tilstrøbt synkutbredels: Ja Tilstrøbt synkmål : 630
 Ekstra Spesifikasjoner : Sertifiseringsorgan :
 Auto % andel af vann ved fi: 100,00

Prøvning

Uttak prøve : Nei Dato : 07-10-2016
 Prøvehypighet :
 Uttak prøve bemerkninger :
 Forprøve gruppenr. : Ingen valgt Foræld. :
 Dato for siste prøve : 21-09-2020 Dato for siste produksjon : 03.12.2020
 Siste forprøve : 45580

Blanderdata

Blander navn	Blandetid	Tommetid	Deltatid	Blander korr.
1 (Blander 1)	40,00	7,00	0,00	0,00
2 (Blander 2)	40,00	7,00	0,00	0,00

Vekt forsinkelse

Blander: Blander 1							
Væekt:	A1-Tilslag 1	A1-Tilslag 2	A1-Pulver	A1-Vann	A1-Kjemi 1	A1-Kjemi 2	A1-Fiber
Sek:	0	0	10	15	16	16	0

Resept flyt synkmål:

Installs:	550	600	650	700
VannBehov:	176,00	179,00	183,00	187,00
Luftinnhold %:	2,00	2,00	2,00	2,00

Tilslag

Materiæler	Synkmål
Alle	
Velde 8-16mm	36,00
Velde 08mm sand	48,00
Velde 02mm fin sand	16,00

Figure A.1: Concrete matrix

Sola Betong

Resept: 251 ~ B35 M45 SKB dmax 16 std FA SI

Tel.: +47 51 64 49 49
W.: @...: post@sola-betong.no

Bindemiddel		Synkmål
Materiale		Alle
Silika		3,30
K-verdi		2,00
Tyrkisk flyveaske		6,00
K-verdi		0,70
Standard sement FA		90,70
K-verdi		1,00

Vann		Procent
Materiale		
varmt vann		
Kaldt vann		100,00

Kjemi		Synkubredningsmål				
Materiale:	Av materiale	Forsinkelse	550	600	650	700
Mapear 25 1:19	% av bindemiddel		0,10	0,10	0,10	0,10
Maepump oil	% av bindemiddel		0,20	0,20	0,20	0,20
Dynamon SX-23	% av bindemiddel	10,00	1,00	1,05	1,10	1,15

Proporsjonering							
Synkubredningsmål	: 200						
Luft	: 2,0						
Ekv. sement	: 346,756						
Samlet vannbehov	: 155,000						
Materialer	Kilo/m ² VO1	Vanninnhold	Kilo/m ²	Pris/Kg	Pris/m ³	CO2/m ²	
Velde 0-16mm	672,184	0,50	675,532	0,1146		2,39	
Velde 08mm send	896,246	1,50	909,556	0,1146		3,18	
Velde 02mm fin send	302,143	1,50	306,613	0,1146		1,07	
Silika	11,274	0,00	11,274	2,9000		0,00	
Tyrkisk flyveaske	20,498	0,00	20,498	0,9735		0,00	
Standard sement FA	309,860	0,00	309,860	0,9155		189,40	
Kaldt vann	152,272	100,00	131,145	0,0000		0,00	
varmt vann	0,000	100,00	0,000	0,0000		0,00	
Mapear 25 1:19	0,342	99,70	0,342	0,7300		0,01	
Maepump oil	0,683	99,10	0,683	6,8000		0,00	
Dynamon SX-23	2,221	77,00	2,221	9,9000		0,00	
	2367,723			2367,723		196,05	

Min/max sementinnhold er anvendt under proporsjoneringen
Proporsjoneringsfell: Prod. synkmål utenfor grenser (500-700)

NS206							
	Resultat	Krav	Ok				
Vannbehov (Fri)	155,000	-					
Effektiv bindemiddel (Fri)	346,756	-					
V/C fri beregning	0,447	-					
Vannbehov (EN206)	155,000	-					
Effektiv Bindemiddel (EN206)	346,756	300,000	✓				
V/C i henhold til EN206	0,447	0,454	✓				
Eff. Bindemiddel mengde fratrukket k	0,000	-					
Bindemiddel (total kg)	341,632	-					
Luft %	2,000	-					
Beregnet m ³	1,000	-					
Kloridinnhold	0,078	0,100	✓				
Andel reaktiv tilslag %	0,000	-					
Alkalinhold	4,384	-					
Flyveaske/bindemiddel forhold	0,223	0,350	✓				
Silika/bindemiddel forhold	0,033	0,110	✓				
Flyveaske, Ren sement andel	70,746	65,000	✓				
Slagg, Ren sement andel	0,000	-					
Matriksvolum eks. luft (l)	383,871	-					
Sementpastavolum (l)	272,323	-					
Samlet vurdering			✓				

Utskrivet d. 26.01.2021 10:48:27 Utskrift nr. 518
System 4009, Side 1.38.22

Side 2 Av 5

Figure A.2: Concrete matrix

Sola Betong

Resept nr. 251 ~ B35 M45 SKB dmax 16 std FA SI

Tel.: +47 51 64 49 49
W...: @...: post@sola-betong.no

BR_A16

Blanket

Resept nr. : 251 ~ B35 M45 SKB dmax 16 std FA SF2
Familie : B
Anvendelse 1 :
Anvendelse 2 :

Klassifikasjon

Bestandighetsklasse : M45 Eksponeringsklasse : X0, XC1, XC2, XC3, XC4, XF1, XD1, XS1,
: B35 Tilstrøbt kons. : XA1, XA2, XA4
Fasthetsklasse : B35
Kontrollklasse : Ingen valgt Ekstra Spesifikasjoner :
Max. Steinstørrelse : 16 Sertifiseringsorgan :

Materiale sammensetning

Forkortelse	Materiale	Densitet Kg/m ³	Mengde Kg/m ³	Volum Liter m ³	Dekl.dato
V16	Valde 8-16mm	2640,000	672,184	254,615	17-10-2016
V08	Valde 08mm sand	2640,000	896,246	339,487	17-10-2016
V02	Valde 02mm fin sand	2670,000	302,143	113,162	17-10-2016
Silika	Silika	2200,000	11,274	5,124	07-10-2016
flyveaske	Tyrisk flyveaske	2300,000	20,498	8,912	07-10-2016
Standard FA	Standard sement FA	3000,000	309,860	103,287	07-10-2016
K-Vann	Kaldt vann	1000,000	152,272	152,272	17-10-2016
V-Vann	varmt vann	1000,000	0,000	0,000	17-10-2016
Luft	Mapearl 25 1:19	1000,000	0,342	0,342	07-10-2016
Pump oil	Maepump oil	1000,000	0,683	0,683	07-10-2016
SX-23	Dynamon SX-23	1050,000	2,221	2,115	07-10-2016
Tilstrøbt luft i betong (2,0 Vol %)				20,000	
			2367,723	1000,000	

Sand	V08	V02 Stein	V16
Materialeklasse		Materialeklasse	
Humus		Lette korn < 2200 kg/m ³	
Kjemisk svind Ml/kg		Lette korn < 2400 kg/m ³	
Innhold av reaktive korn		Lette korn < 2500 kg/m ³	
Merteleksjon % Uge		Kritisk absorpsjon av 10 Pct.	
Acc. merteleksjon % Ug		Acc. merteleksjon % Ug	
Absorpsjon %	1,00	1,40 Absorpsjon %	0,40
DLower		DLower	
DUpper		DUpper	

Sement	Sulfatres.
Standard sement FA	Nei

Andre tilsetninger	Tilsetningsstoffer	Luft	Pump oil	SX-23
Tørstoffinnhold %	Tørstoffinnhold %	0,30	0,90	23,00

Fibre	Vann	K-Vann	V-Vann
Type	Materialeklasse		
Fiber tverrsnit	Tørstoffinnhold %	0,00	0,00
Fiber lengde			

Klorid/Alkali regnskab	Innhold av delmaterialer	Kg/m ³	Kloridberegning		Alkaliberegning	
			% cl	Kg/m ³	% Ekv. Alk	Kg/m ³
	Valde 8-16mm	672,184	0,000	0,000		
	Valde 08mm sand	896,246	0,000	0,000		
	Valde 02mm fin sand	302,143	0,000	0,000		
	Silika	11,274	0,000	0,000	0,000	0,000
	Tyrisk flyveaske	20,498	0,000	0,000	0,000	0,000
	Standard sement FA	309,860	0,085	0,263	1,400	4,338
	Kaldt vann	152,272	0,000	0,000	0,000	0,000
	varmt vann	0,000	0,000	0,000	0,000	0,000
	Mapearl 25 1:19	0,342	0,050	0,000	0,200	0,001
	Maepump oil	0,683	0,050	0,000	0,100	0,001
	Dynamon SX-23	2,221	0,050	0,001	2,000	0,044
	Total			0,265		4,384

Utskrivet d. 26.01.2021 10:48:27 Utskrift nr. 518
System 4009, Build 1.38.22

BR_A16

Side 3 Av 5

Figure A.3: Concrete matrix

Tel.: +47 51 64 49 49
 W...: - @...: post@sola-betong.no

Kornkurver, gjennomgang i %				
	V16	V08	V02	Total
Mengde, Kg	672,184	896,246	302,143	1870,573
Vol.-%	36,000	48,000	16,000	100,000
Sikt, mm				
64,000	100,000	100,000	100,000	100,000
32,000	100,000	100,000	100,000	100,000
16,000	99,324	100,000	100,000	99,757
8,000	89,654	97,800	100,000	95,220
4,000	78,578	75,300	100,000	80,432
2,000	67,461	63,300	94,000	69,710
1,000	56,313	45,600	71,000	53,521
0,500	45,138	29,700	50,000	38,506
0,250	33,934	16,900	32,000	25,446
0,125	22,699	9,400	19,300	15,772
0,063	11,425	5,300	10,000	8,257
0,000	0,000	0,000	0,000	0,000

Siktekurve

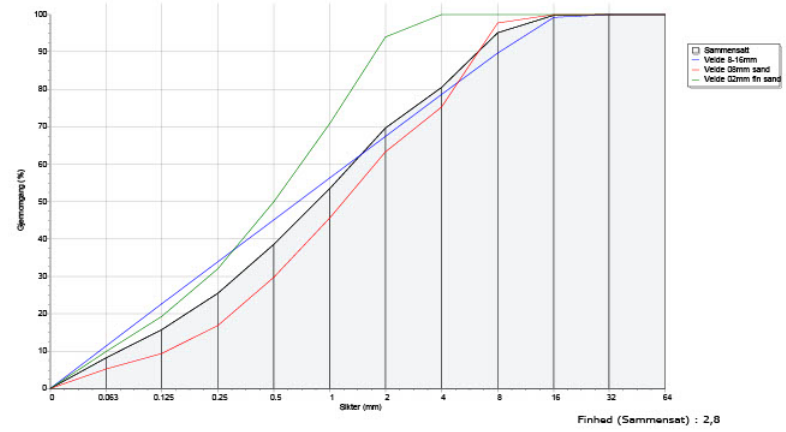


Figure A.4: Concrete matrix

Prøvedata

Flg nr.	Datetid	Luft %	Konsistens	V/C forhold	T 2	T 7	T 28
48887	21-09-2020 09:04	2,00/0,00	580/640	0,447/0,444/0,000	0,0	0,0	60,0/61,6
47705	20-08-2020 12:21	2,00/0,00	630/640	0,447/0,447/0,000	0,0	0,0	60,0/64,0
45630	19-06-2020 09:00	2,00/0,00	630/630	0,447/0,447/0,000	0,0	0,0	60,0/53,4
45580	18-06-2020 10:42	2,00/0,00	630/640	0,447/0,448/0,444	0,0	0,0	60,0/59,1
43021	21-04-2020 11:30	2,00/0,00	630/680	0,447/0,448/0,444	0,0	0,0	60,0/60,6
40123	13-02-2020 14:42	2,00/0,00	630/650	0,447/0,452/0,451	0,0	0,0	60,0/56,5
36958	13-11-2019 08:28	2,00/0,00	630/660	0,447/0,457/0,451	0,0	0,0	60,0/57,5
32746	04-07-2019 11:36	2,00/0,00	630/660	0,447/0,447/0,000	0,0	0,0	60,0/62,1
32549	01-07-2019 13:12	2,00/0,00	630/640	0,447/0,450/0,451	0,0	0,0	60,0/66,2
31139	03-06-2019 07:01	2,00/0,00	630/630	0,447/0,449/0,000	0,0	0,0	60,0/64,7
Gennemsnit		0,00/0,00	625/646	0,447/0,449/0,451	0,0	0,0	60,0/60,6

Figure A.5: Concrete matrix

MAPEI

Dynamon SX-23

Superplastiserende tilsetningsstoff til betong og mørtel

PRODUKTBESKRIVELSE
 Dynamon SX-23 er et svært effektivt superplastiserende tilsetningsstoff basert på modifiserte akrylpolymerer. Produktet tilhører Dynamon-systemet som er basert på DPP-teknologi, Designed Performance Polymers, utviklet av Mapei, hvor tilsetningsstoffenes egenskaper skræddersys til forskjellige betongtyper. Dynamon-systemet er utviklet på grunnlag av Mapeis egen sammensetning og produksjon av monomerer.

BRUKSOMRÅDE
 Dynamon SX-23 er spesielt utviklet til ferdigbetongproduksjon og brukes i alle betongtyper for å gjøre betongen enklere å bearbeide og/eller redusere vannbehovet.

Noen spesielle bruksområder er:

- Vannrett betong med krav om høy eller svært høy styrke, og med strenge krav til betongens holdbarhet i aggressive miljøer.
- Betong med særlige krav til høy støpelighet.
- Selvkomprimerende betong med noe lengre åpentid. Om nødvendig kan denne betongtypen stabiliseres med et viskositetsøkende tilsetningsstoff av type **Viscofluid** eller **Viscostar**.
- Frostbestandig betong – ved kombinasjon med et luftinnførende tilsetningsstoff – type **Mapeair**.

Typen av luftinnførende tilsetningsstoff gjøres ut fra tilgjengelig kunnskap om de andre delmaterialenes egenskaper.

- Gulvbetong for å oppnå en smidig betong med forbedret støpelighet. Høye doseringer og lave temperaturer kan medføre en viss retardering av betongen.

Dynamon SX-23 skiller seg vesentlig fra superplastiserende tilsetningsstoffer basert på sulfonerte melaminer og naffalener samt fra første generasjons akrylbaserte polymerer, ved en betydelig høyere vannreducerende effekt og økt åpentid. Nødvendig dosering for ønsket bearbeidingsveie/ vannreduksjon vil være vesentlig lavere med **Dynamon SX-23** enn med eldre typer superplastiserende tilsetningsstoffer.

Doseringstidspunktet for **Dynamon SX-23** er ikke så viktig, men kortest blandetid oppnås ved tilsetning av **Dynamon SX-23** etter tilsetning av minst 80 % av blandedvannet. Også her er det viktig å foreta en utprøving for optimal utnyttelse av aktuelt blandedustyr.

EGENSKAPER
 Dynamon SX-23 er en vannoppløsning av aktive akrylpolymerer som effektivt dispergerer sementen i blandingen.

Denne effekten kan utnyttes på tre måter:

Figure A.6: Dynamon SX-23 Superplasticizer

A.2 Superplasticizers

B Test protocols

B.1 Young's Modulus

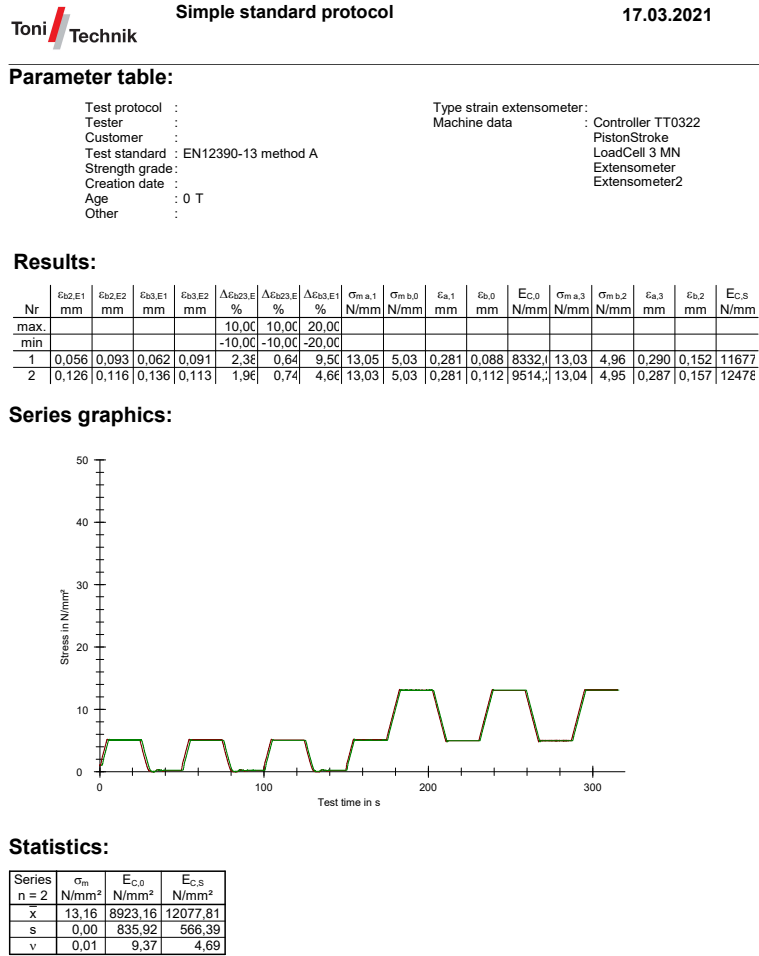


Figure B.1: Young's modulus

B.2 Compression test

Parameter table:

Test protocol : Test Bachelor
Tester : Daniel og Yousef
Customer :
Test standard :
Strength grade :
Other :
Type strain extensometer :
Machine data : Controller TT1412
PistonStroke
LoadCell 3 MN

Results:

Nr	Date	ID	F _m kN	Clock time	σ _m N/mm ²
1	17.03.2021	Nr.1 Terning	546,66	13.40.28	54,67
2	17.03.2021	Nr.2 Terning	685,25	13.44.31	68,52
3	17.03.2021	Nr.3 Terning	696,64	13.48.29	69,66
5	17.03.2021	Nr.1 Sylinder	695,58	13.55.42	39,36
6	17.03.2021	Nr.2 Sylinder	726,18	14.01.29	41,09
7	17.03.2021	Nr.3 Sylinder	749,17	14.04.56	42,39

Series graphics:

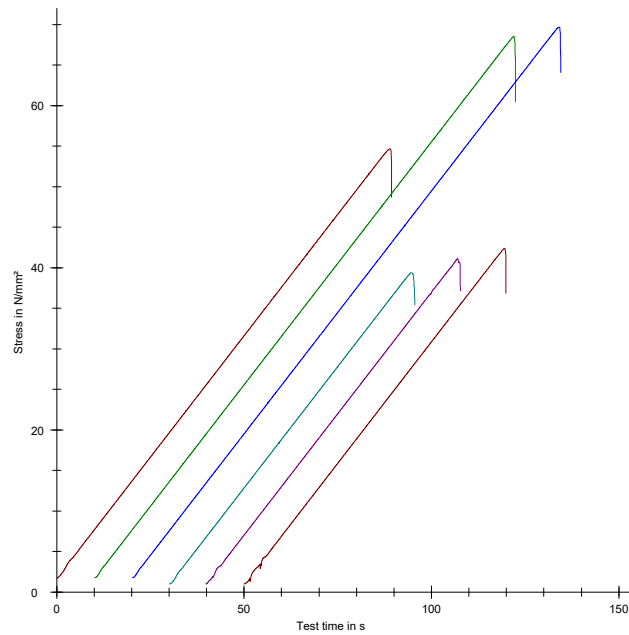


Figure B.2: Compression test

B.3 Splitting tensile test

Parameter table:

Test protocol	: UHPC	Type strain extensometer:	
Tester	: Fredrik Knutsen	Machine data	: Controller TT1412
Customer	:		: PistonStroke
Test standard	:		: LoadCell 3 MN
Strength grade	:		
Other	:		

Results:

Nr	Date	ID	F _m kN	Clock time
1	17.03.2021	AniFa_28dg	238,95	14.12.58
2	17.03.2021	AniFa_28dg #2	190,07	14.16.36

Series graphics:

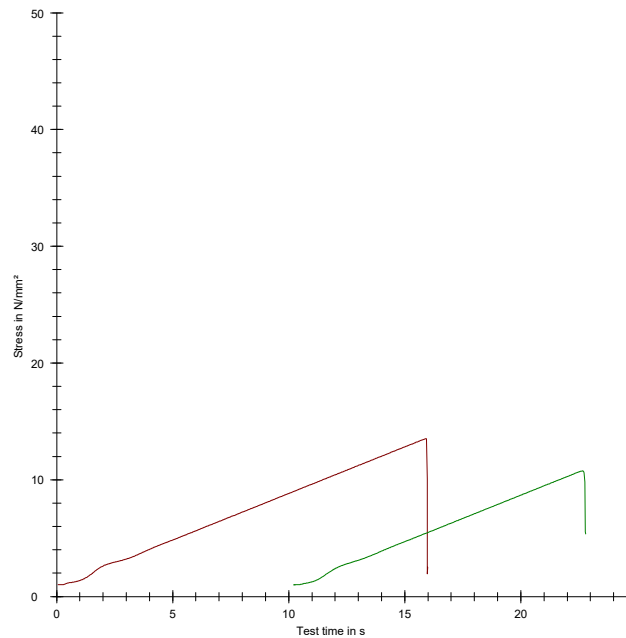


Figure B.3: Splitting tensile test

B.4 Applied forces at IKM

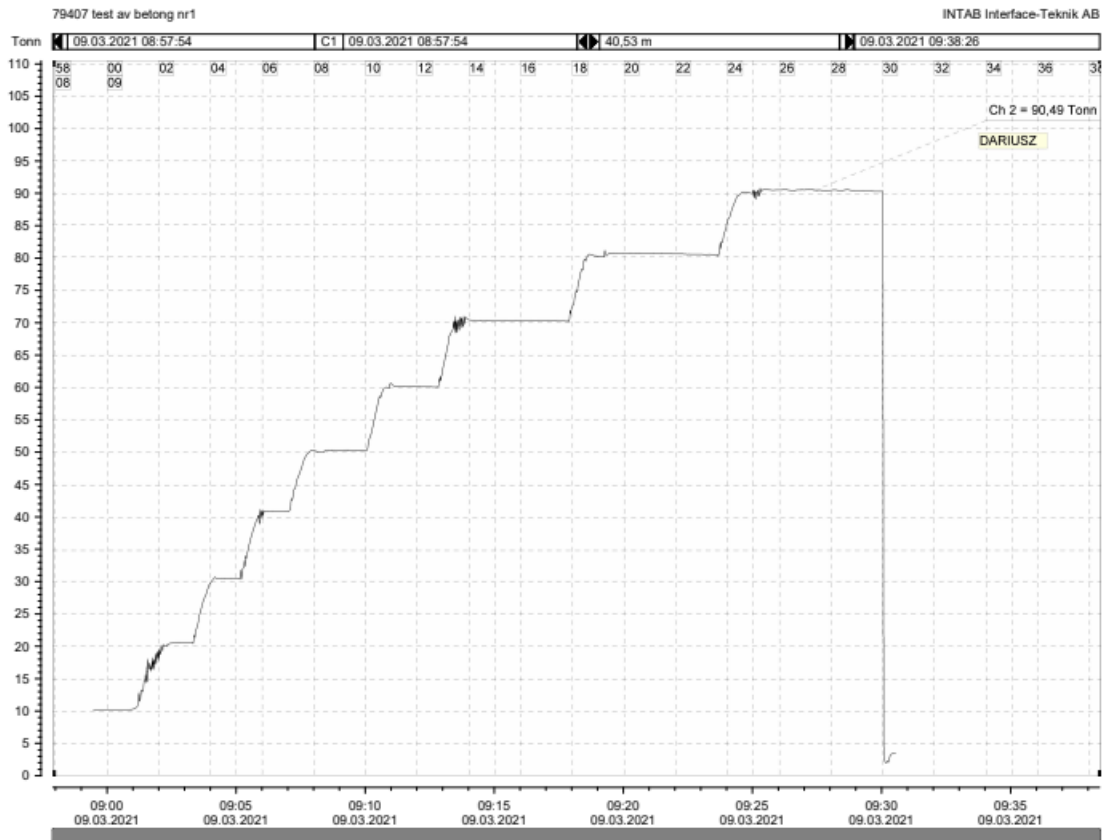


Figure B.4: Load applied beam 1

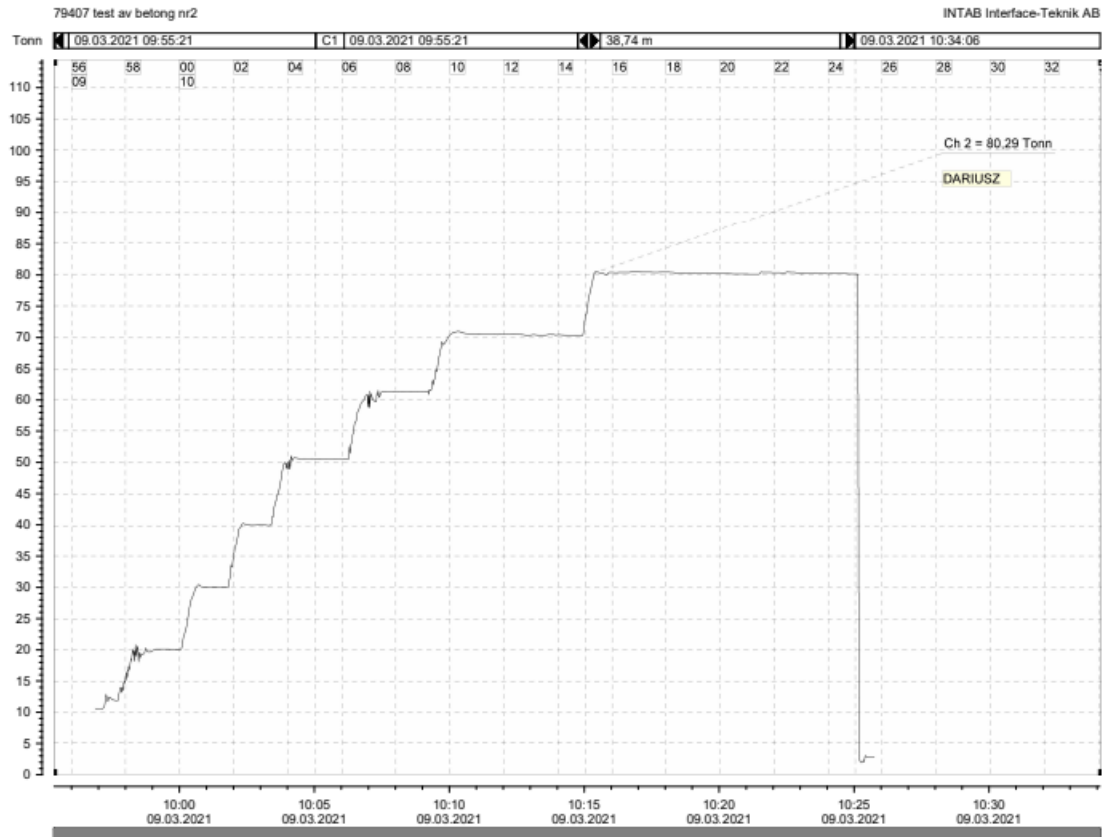


Figure B.5: Load applied on beam 2

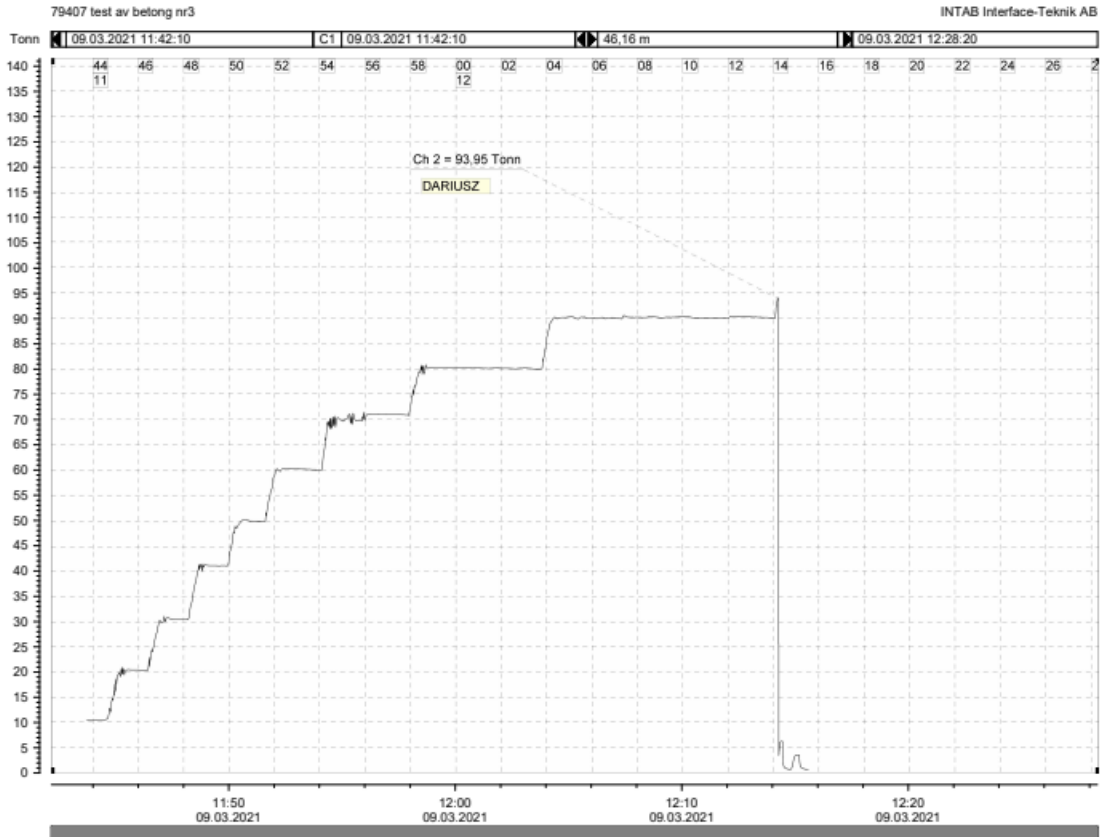


Figure B.6: Load applied on beam 3

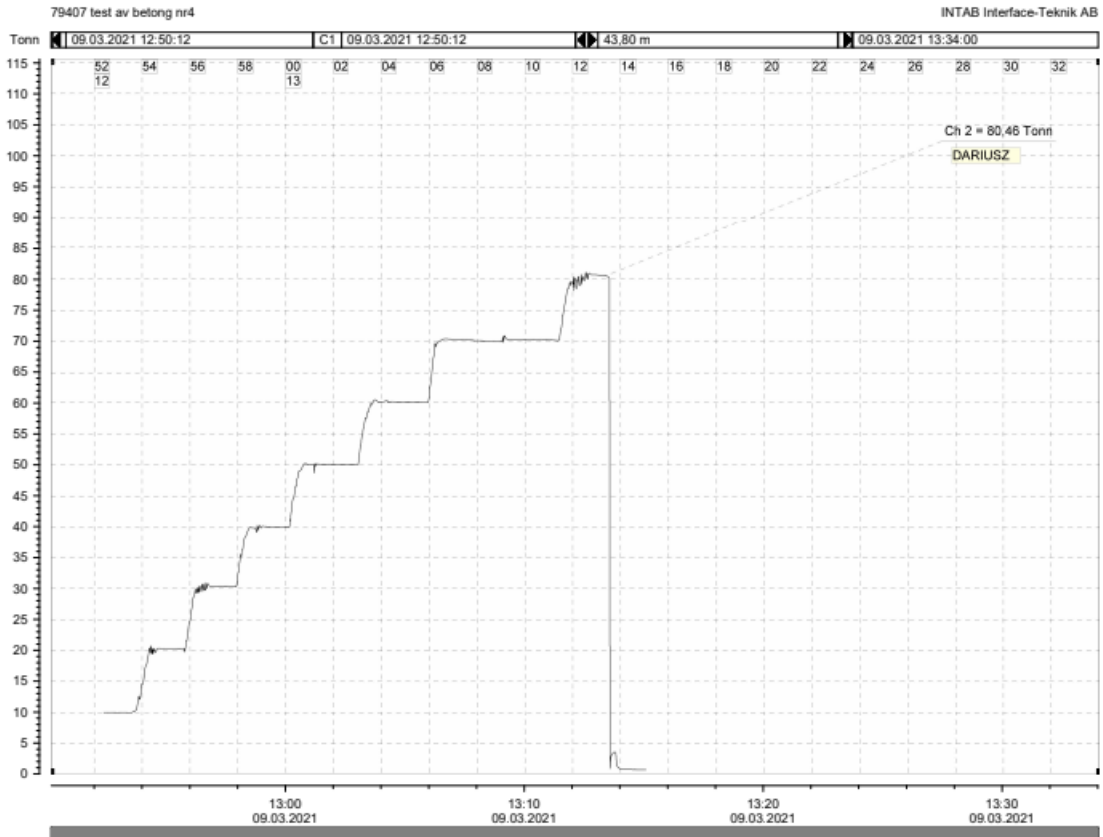


Figure B.7: Load applied on beam 4

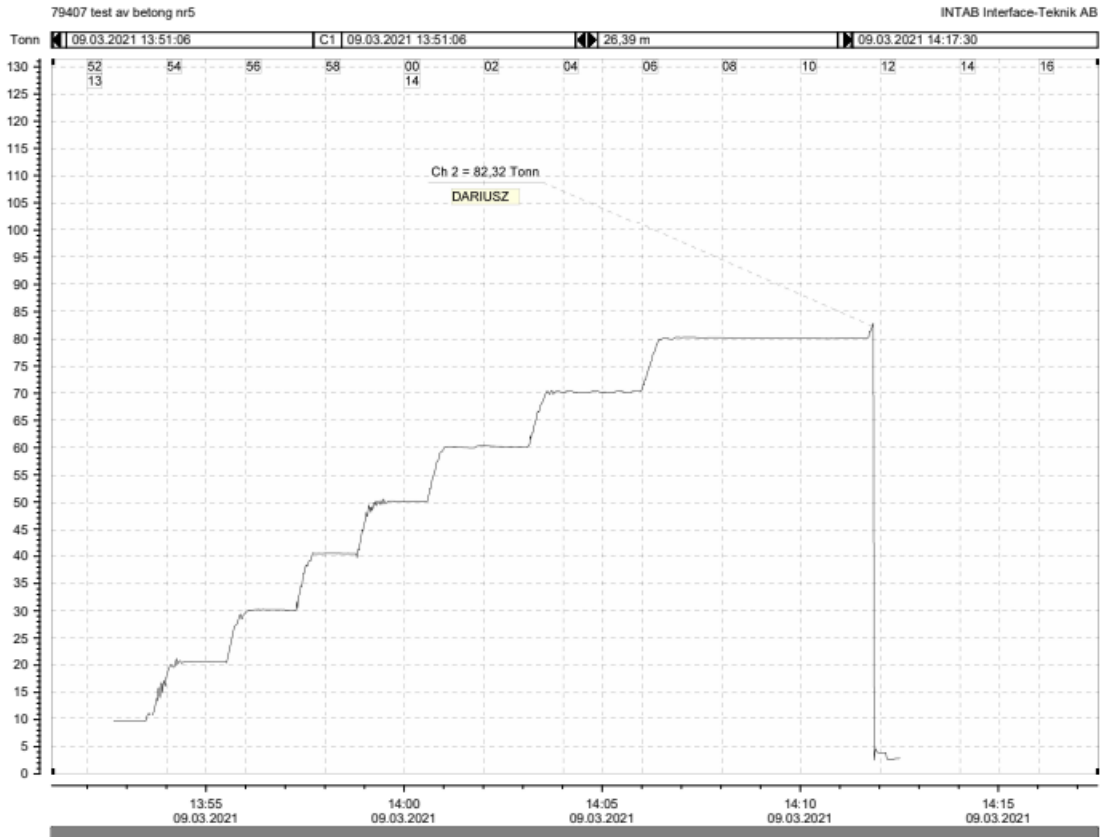


Figure B.8: Load applied on beam 5

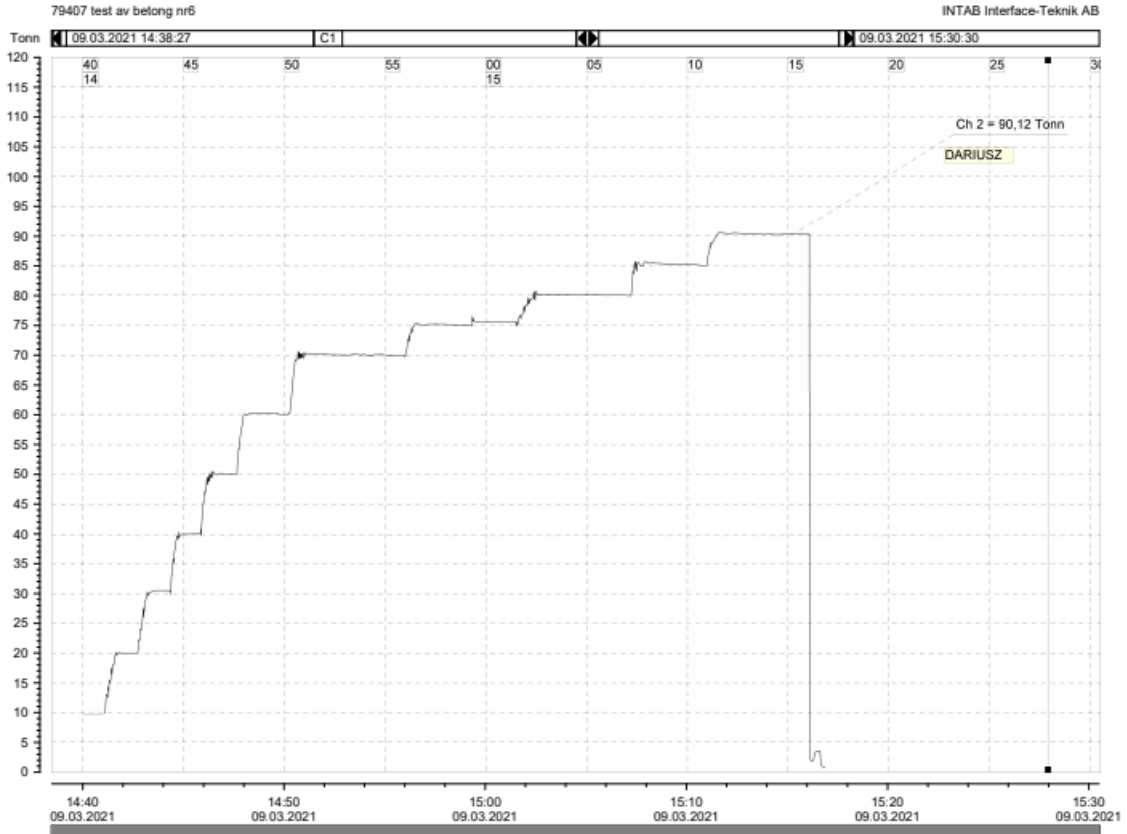


Figure B.9: Load applied on beam 6

B.5 Crack spacing results

Beam 1 Side 1					Beam 1 Side 2				
Crack	Rebar 1	Spacing	Rebar 2	Spacing2	Crack	Rebar 1	Spacing	Rebar 2	Spacing2
	0		0			0		0	
1	191	191	192	192	1	207	207	184	184
2	370	179	377	185	2	430	223	422	238
3	579	209	608	231	3	575	145	794	372
4	810	231	810	202	4	798	223	1116	322
5	1100	290	1111	301	5	1099	301	1249	133
6	1300	200	1277	166	6	1253	154	1515	266
7	1532	232	1521	244	7	1507	254	1719	204
8	1779	247	1751	230	8	1738	231	2000	281
9	2000	221	2000	249	9	2000	262		
Minimum		179		166	Minimum		145		133
Maximum		290		301	Maximum		301		372
Average		222.222222		222.222222	Average		222.222222		250

Beam 1 Side 3					Beam 1 Side 4				
Crack	Rebar 1	Spacing	Rebar 2	Spacing2	Crack	Rebar 1	Spacing	Rebar 2	Spacing2
	0		0			0		0	
1	248	248	267	267	1	184	184	184	184
2	500	252	498	231	2	361	177	349	165
3	766	266	704	206	3	502	141	503	154
4	917	151	926	222	4	815	313	817	314
5	1199	282	1194	268	5	1140	325	1079	262
6	1432	233	1431	237	6	1296	156	1304	225
7	1577	145	1810	379	7	1527	231	1507	203
8	1794	217	2000	190	8	1742	215	1738	231
9	2000	206			9	2000	258	2000	262
Minimum		145		190	Minimum		141		154
Maximum		282		379	Maximum		325		314
Average		222.222222		250	Average		222.222222		222.222222

Figure B.10: Crack spacing - beam 1

Beam 1 Side 1					Beam 1 Side 2				
Crack	Rebar 1	Spacing	Rebar 2	Spacing2	Crack	Rebar 1	Spacing	Rebar 2	Spacing2
	0		0			0		0	
1	191	191	192	192	1	207	207	184	184
2	370	179	377	185	2	430	223	422	238
3	579	209	608	231	3	575	145	794	372
4	810	231	810	202	4	798	223	1116	322
5	1100	290	1111	301	5	1099	301	1249	133
6	1300	200	1277	166	6	1253	154	1515	266
7	1532	232	1521	244	7	1507	254	1719	204
8	1779	247	1751	230	8	1738	231	2000	281
9	2000	221	2000	249	9	2000	262		
Minimum		179		166	Minimum		145		133
Maximum		290		301	Maximum		301		372
Average		222.222222		222.222222	Average		222.222222		250

Beam 1 Side 3					Beam 1 Side 4				
Crack	Rebar 1	Spacing	Rebar 2	Spacing2	Crack	Rebar 1	Spacing	Rebar 2	Spacing2
	0		0			0		0	
1	248	248	267	267	1	184	184	184	184
2	500	252	498	231	2	361	177	349	165
3	766	266	704	206	3	502	141	503	154
4	917	151	926	222	4	815	313	817	314
5	1199	282	1194	268	5	1140	325	1079	262
6	1432	233	1431	237	6	1296	156	1304	225
7	1577	145	1810	379	7	1527	231	1507	203
8	1794	217	2000	190	8	1742	215	1738	231
9	2000	206			9	2000	258	2000	262
Minimum		145		190	Minimum		141		154
Maximum		282		379	Maximum		325		314
Average		222.222222		250	Average		222.222222		222.222222

Figure B.11: Crack spacing - beam 2

Beam 3 Side 1					Beam 3 Side 2				
Crack	Rebar 1	Spacing	Rebar 2	Spacing2	Crack	Rebar 1	Spacing	Rebar 2	Spacing2
	0		0			0		0	
1	333	333	223	223	1	202	202	196	196
2	431	98	330	107	2	414	212	295	99
3	599	168	446	116	3	593	179	402	107
4	735	136	581	135	4	811	218	599	197
5	809	74	695	114	5	954	143	684	85
6	971	162	832	137	6	1172	218	807	123
7	1196	225	983	151	7	1359	187	956	149
8	1379	183	1202	219	8	1489	130	1165	209
9	1457	78	1698	496	9	1690	201	1358	193
10	1661	204	2000	302	10	2000	310	1483	125
11	2000	339						1696	213
Minimum			74	107				2000	304
Maximum			339	496	Minimum		130		85
Average		181.81818		200	Maximum		310		304
					Average		200		166.66667
Beam 3 Side 3					Beam 3 Side 24				
Crack	Rebar 1	Spacing	Rebar 2	Spacing2	Crack	Rebar 1	Spacing	Rebar 2	Spacing2
	0		0			0		0	
1	211	211	208	208	1	220	220	189	189
2	409	198	415	207	2	315	95	311	122
3	586	177	604	189	3	418	103	419	108
4	726	140	733	129	4	596	178	601	182
5	962	236	965	232	5	713	117	736	135
6	1172	210	1181	216	6	965	252	969	233
7	1451	279	1481	300	7	1160	195	1186	217
8	1659	208	1653	172	8	1447	287	1463	277
9	2000	341	2000	347	9	1666	219	1655	192
10					10	2000	334	2000	345
11									
Minimum		140		129					
Maximum		341		347	Minimum		95		108
Average		222.22222		222.22222	Maximum		334		345
					Average		200		200

Figure B.12: Crack spacing - beam 3

Beam 4 Side 4					Beam 4 Side 2				
Crack	Rebar 1	Spacing	Rebar 2	Spacing2	Crack	Rebar 1	Spacing	Rebar 2	Spacing2
	0		0			0		0	
1	170	170	170	170	1	162	162	190	190
2	386	216	335	165	2	354	192	341	151
3	557	171	611	276	3	618	264	630	289
4	784	227	784	173	4	791	173	789	159
5	1018	234	993	209	5	992	201	973	184
6	1166	148	1159	166	6	1145	153	1132	159
7	1345	179	1315	156	7	1230	85	1281	149
8	1415	70	1420	105	8	1423	193	1419	138
9	1538	123	1552	132	9	1559	136	1547	128
10	1659	121	1672	120	10	1665	106	1689	142
11	1772	113	1814	142	11	1811	146	1834	145
12	2000	228	2000	186	12	2000	189	2000	166
Minimum		70		105	Minimum		85		128
Maximum		234		276	Maximum		264		289
Average		166.6666667		166.6666667	Average		166.6666667		166.6666667

Beam 3 Side 3					Beam 4 Side 4				
Crack	Rebar 1	Spacing	Rebar 2	Spacing2	Crack	Rebar 1	Spacing	Rebar 2	Spacing2
	0		0			0		0	
1	182	182	178	178	1	350	350	170	170
2	346	164	347	169	2	593	243	335	165
3	614	268	588	241	3	792	199	611	276
4	785	171	780	192	4	1005	213	784	173
5	1026	241	993	213	5	1139	134	993	209
6	1135	109	1136	143	6	1304	165	1159	166
7	1264	129	1295	159	7	1424	120	1315	156
8	1413	149	1410	115	8	1556	132	1420	105
9	1696	283	1542	132	9	1674	118	1552	132
10	2000	304	1661	119	10	1875	201	1672	120
			1864	203	11	2000	125	2000	328
			2000	136					
Minimum		109		115	Minimum		118		105
Maximum		304		241	Maximum		350		328
Average		200		169.4545455	Average		181.8181818		181.8181818

Figure B.13: Crack spacing - beam 4

Beam 5 Side 1					Beam 5 Side 1				
Crack	Rebar 1	Spacing	Rebar 2	Spacing2	Crack	Rebar 1	Spacing	Rebar 2	Spacing2
	0		0			0		0	
1	227	227	223	223	1	199	199	223	223
2	390	163	627	404	2	357	158	378	155
3	560	170	759	132	3	542	185	539	161
4	773	213	970	211	4	780	238	784	245
5	935	162	1205	235	5	1051	271	1039	255
6	1180	245	1444	239	6	1237	186	1241	202
7	1365	185	1764	320	7	1404	167	1466	225
8	1475	110	2000	236	8	1646	242	1657	191
9	1663	188			9	1778	132	1770	113
10	1772	109			10	2000	222	2000	230
11	2000	228							
Minimum		109		132	Minimum		132		113
Maximum		245		404	Maximum		271		255
Average		181.818182		250	Average		200		200

Beam 5 Side 3					Beam 5 Side 4				
Crack	Rebar 1	Spacing	Rebar 2	Spacing2	Crack	Rebar 1	Spacing	Rebar 2	Spacing2
	0		0			0		0	
1	204	204	202	202	1	198	198	169	169
2	350	146	362	160	2	354	156	361	192
3	559	209	553	191	3	554	200	625	264
4	783	224	789	236	4	781	227	745	120
5	976	193	985	196	5	987	206	976	231
6	1052	76	1077	92	6	1066	79	1061	85
7	1234	182	1241	164	7	1245	179	1236	175
8	1401	167	1406	165	8	1422	177	1439	203
9	1647	246	1631	225	9	1625	203	1614	175
10	1775	128	1778	147	10	1784	159	1775	161
11	2000	225	2000	222	11	2000	216	2000	225
Minimum		76		92	Minimum		79		85
Maximum		246		236	Maximum		227		264
Average		181.818182		181.818182	Average		181.818182		181.818182

Figure B.14: Crack spacing - beam 5

Beam 6 Side 1					Beam 6 Side 2				
Crack	Rebar 1	Spacing	Rebar 2	Spacing2	Crack	Rebar 1	Spacing	Rebar 2	Spacing2
	0		0			0		0	
1	200	200	164	164	1	168	168	194	194
2	403	203	456	292	2	390	222	358	164
3	769	366	750	294	3	533	143	517	159
4	931	162	930	180	4	795	262	780	263
5	1365	434	1198	268	5	920	125	965	185
6	2000	635	1416	218	6	1172	252	1178	213
7			1667	251	7	1416	244	1494	316
8			1805	138	8	1500	84	1703	209
9			2000	195	9	1662	162	1800	97
10					10	1799	137	2000	200
11					11	2000	201		
12					12				
Minimum		162		138	Minimum		84		97
Maximum		635		294	Maximum		262		316
Average		333.333333		222.222222	Average		181.818182		200

Beam 6 Side 1					Beam 6 Side 4				
Crack	Rebar 1	Spacing	Rebar 2	Spacing2	Crack	Rebar 1	Spacing	Rebar 2	Spacing2
	0		0			0		0	
1	197	197	164	164	1	184	184	192	192
2	376	179	456	292	2	382	198	373	181
3	579	203	750	294	3	611	229	585	212
4	794	215	930	180	4	779	168	788	203
5	958	164	1198	268	5	935	156	944	156
6	1169	211	1416	218	6	1170	235	1169	225
7	1388	219	1667	251	7	1361	191	1381	212
8	1504	116	1805	138	8	1698	337	1510	129
9	1706	202	2000	195	9	1805	107	1702	192
10	1808	102			10	2000	195	1805	103
11	2000	192						2000	195
12									
Minimum		102		138	Minimum		107		103
Maximum		219		294	Maximum		337		225
Average		181.818182		222.222222	Average		200		181.818182

Figure B.15: Crack spacing - beam 6

C Order and design of load connections

C.1 Order of load connections

Order load connection

From NorskstaaI.no

HEB 1000 S355 steel. Produktgruppe 5223.

We need 900 mm. To be on the safer side, order around 1200 mm – 1500mm.

We use both flanges of the beam. Cut at middle (at 500 mm)

From workshop at UIS

First order from workshop will be:

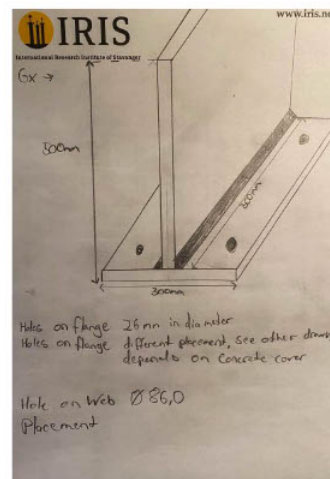
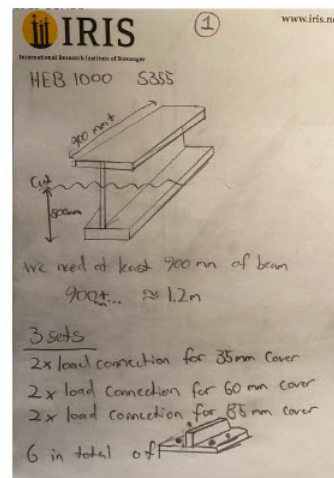
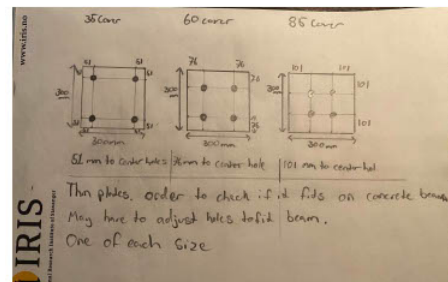
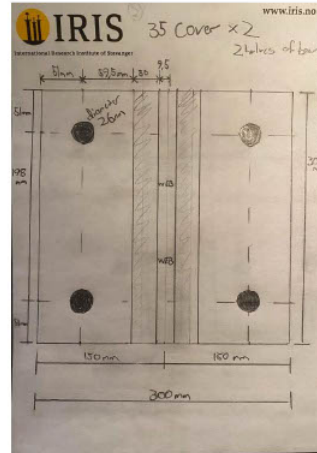
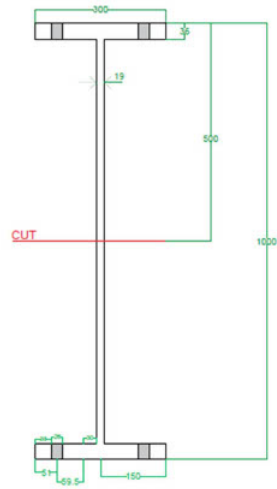


Figure C.1: Complete order of load connections

35 mm cover



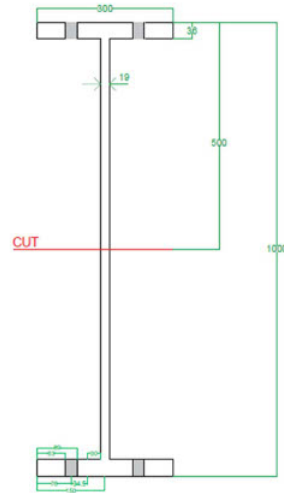
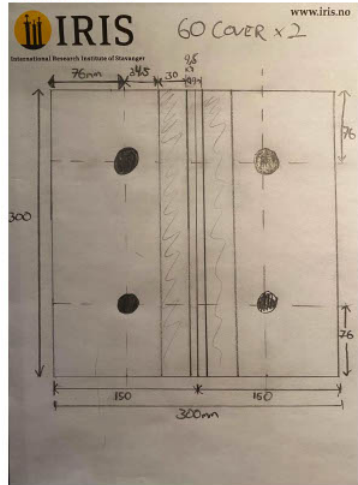
Center of holes at 51 mm from each side.

Hole diameter 26 mm

Cut beam in half at the height 500 mm. With the two halves we can complete the set

Figure C.2: Complete order of load connections

60 mm Cover



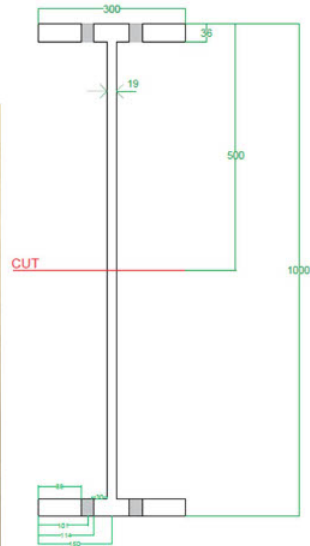
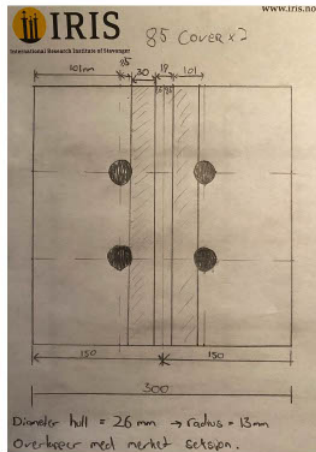
Center of holes at 76 mm from each side.

Hole diameter 26 mm

Cut beam in half at the height 500 mm. With the two halves we can complete the set for 60mm cover

Figure C.3: Complete order of load connections

85 mm Cover



Center of holes at 101 mm from each side.

Hole diameter 26 mm

Cut beam in half at the height 500 mm. With the two halves we can complete the set for 85mm cover

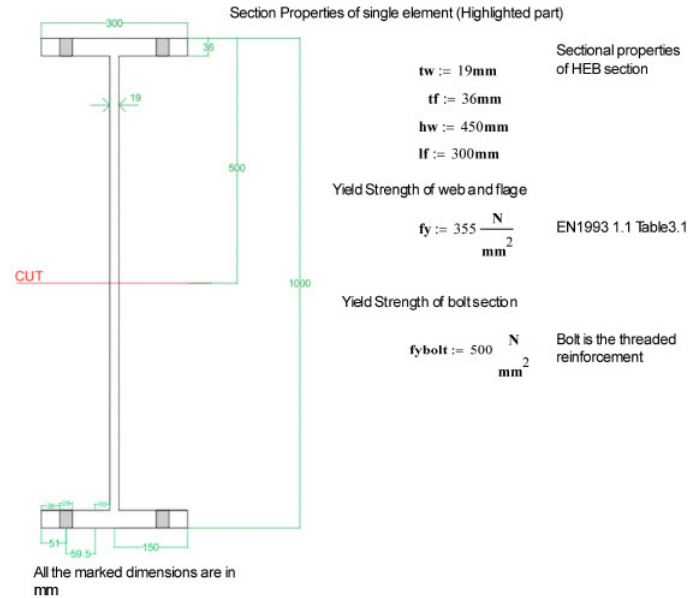
The holes in flange overlap with the welded section between flange and beam. Have to make sure the nut will fit, might have to remove some of the weld.

Figure C.4: Complete order of load connections

C.2 Design of load connections

Design calculation of the New loading connection at IKM test

HEB S355 1000



Resistance of T-Stub - Step 1A

n := 51mm m1 := 59.5mm

EN1993 1.8 Table 6.2

e1 := 51mm
dw := 41.6mm

EN1993 1.8 Table 6.4 and M24 nut properties end to end diameter of nut

For a circular failure pattern

End $l_{eff1} := 2 \cdot 3.14159 \cdot m1 = 373.849 \cdot \text{mm}$
bolt $l_{eff1} := 3.14159m1 + 2 \cdot e1 = 288.925 \cdot \text{mm}$

EN1993 1.8 Table 6.4 (Unstiffened case)

For a non-circular failure pattern

End $l_{eff2} := 4 \cdot m1 + 1.25 \cdot n = 0.302 \text{ m}$
bolt $l_{eff2} := 2m1 + 0.625 \cdot e1 + e1 = 0.202 \text{ m}$

Figure C.5: Design of 35 mm load connection part 1/9

$$ew := \frac{dw}{4} = 0.01 \text{ m}$$

$$\gamma_{M0} := 1 \quad \text{EN1993 1.1 NA2.15}$$

$$\gamma_{M1} := 1$$

$$dboltm := \frac{(24.84\text{mm} + 23.16\text{mm})}{2} = 0.024 \text{ m}$$

$$FtRd := 3.14 \cdot \left(\frac{dboltm}{2}\right)^2 \cdot fybolt = 226.08 \cdot \text{kN} \quad \text{EN1993 1.8 Table 6.2 (Design resistance for T-stub flange)}$$

$$Mpl1Rd := \frac{0.25 \cdot leff11 \cdot tf^2 \cdot fy}{\gamma_{M0}} = 3.323 \times 10^4 \cdot \text{m} \cdot \text{N} \quad \text{Lesser of leff1 or leff11}$$

$$Mpl2Rd := \frac{0.25 \cdot leff22 \cdot tf^2 \cdot fy}{\gamma_{M0}} = 2.322 \times 10^4 \cdot \text{N} \cdot \text{m} \quad \text{Lesser of leff2 or leff22}$$

Mode 1 failure - Complete flange yielding

$$Ft1Rd := \frac{(8 \cdot n - 2ew) \cdot Mpl1Rd}{2 \cdot m1 \cdot n - ew \cdot (m1 + n)} = 2.615 \times 10^6 \text{ m}^{-1} \cdot \text{N} \cdot \text{m}$$

Mode 2 Failure - Bolt failure with flange yielding

$$Ft2Rd := \frac{2 \cdot Mpl2Rd + n \cdot FtRd \cdot 4}{m1 + n} = 8.376 \times 10^5 \text{ m}^{-1} \cdot \text{N} \cdot \text{m}$$

Mode3 Failure - Bolt Failure

$$Ft3Rd := 4 \cdot FtRd = 9.043 \times 10^5 \cdot \text{N}$$

Resistance of flange

Minimum of Ft1Rd, Ft2Rd, Ft3Rd

$$Ft2Rd = 8.376 \times 10^5 \cdot \text{N}$$

Figure C.6: Design of 35 mm load connection part 2/9

Check for Beam Web tension - Step 1B

EN1993 1.8 Section 6.2.6.8

$$\text{beffweb} := 300\text{mm} - 86\text{mm} = 0.214\text{m}$$

EN1993 1.8 Section 6.2.6.8 suggest to use Fig.6.10 and Table 6.6

$$\text{twb} := \text{tw} = 19 \cdot \text{mm}$$

Consider the combined section

$$\text{fywb} := 355 \frac{\text{N}}{\text{mm}^2}$$

Web tensile Capacity

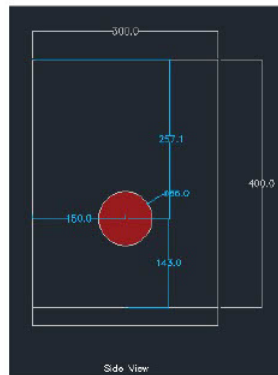
$$\text{FtwbRd} := \frac{\text{beffweb} \cdot \text{twb} \cdot \text{fywb}}{\gamma \text{M0}} = 1.443 \times 10^3 \cdot \text{kN}$$

EN1993 1.8 in Eq 6.22

Shear failure can occur at the loading shackle connection

Ref:

<https://www.machinedesign.com/fasteners/what-s-difference-between-bearing-shear-and-tear-out-stress>



$$\text{Ashear} := 2 \cdot 257\text{mm} \cdot \text{tw} = 9.766 \times 10^{-3} \text{m}^2$$

Figure C.7: Design of 35 mm load connection part 3/9

$$f_{\text{shear}} := 0.6 \cdot f_{ywb} = 2.13 \times 10^8 \frac{\text{N}}{\text{m}^2}$$

$$F_{\text{shearRD}} := A_{\text{shear}} \cdot f_{\text{shear}} = 2.08 \times 10^6 \text{ Pa}$$

Tearout Failure of web

Ref:
<https://www.machinedesign.com/fasteners/what-s-difference-between-bearing-shear-and-tear-out-stress>

To prevent tear-out, it is suggested that the distance from the edge of the material to the edge of the hole be at least equal to the diameter of the hole

Therefore No tearout fail occur

Verification of nut and bolt connection

Nut Strength Verification

The bolt is considered as the threaded end of reinforcement and the nut is selected as M24 strength class 8.

Tensile strength of 4 bolt set

$$F_{t3Rd} = 9.043 \times 10^5 \cdot \text{N}$$

Refer sheet No.2

Verification for the thread stripping before tensile failure of bolts

Tensile strength of one bolt

$$F_{\text{bolt}} := \frac{F_{t3Rd}}{4} = 2.261 \times 10^5 \cdot \text{N}$$

Figure C.8: Design of 35 mm load connection part 4/9

Shear strength of bolt from the reinforcement

$$F_{\text{shearbolt}} = 0.85 \cdot f_{\text{ybolt}} = 425 \cdot \text{MPa}$$

0.85 is the EC2 factor used when calculating shear links

Calculation of effective length

$$A_{\text{shearbolt}} := \frac{F_{\text{bolt}}}{F_{\text{shearbolt}}} = 5.32 \times 10^{-4} \cdot \text{m}^2$$

$$L_{\text{effshear}} := \frac{A_{\text{shearbolt}}}{3.14 \cdot d_{\text{boltm}}} = 7.059 \times 10^{-3} \cdot \text{m}$$

In order to hold the Tensile strength of a bolt required length is

$$L_{\text{effshear}} = 7.059 \times 10^{-3} \cdot \text{m}$$

Reference
www.tribology-abc.com

http://www.tribology-abc.com/calculators/e3_6e.htm

Thread stripping strength of bolt (reinforcement) $F_{\text{threadbolt}}$

Reference :
<http://www.tribology-abc.com/sub9.htm>

Length of engagement

$$L_{\text{eng}} := 0.75 \cdot 24\text{mm} = 0.018 \cdot \text{m}$$

Assume only one nut is used

$$A_{\text{engshear}} := 3.14 \cdot d_{\text{boltm}} \cdot L_{\text{eng}} = 1.356 \times 10^{-3} \cdot \text{m}^2$$

$$F_{\text{threadbolt}} := A_{\text{engshear}} \cdot F_{\text{shearbolt}} = 5.765 \times 10^5 \cdot \text{N}$$

Thread stripping does not occur before Tensile strength of bolt

Figure C.9: Design of 35 mm load connection part 5/9

Verification for the thickness of flange (steel plate connected to bolts)

Tensile Strength verification



cross section of steel plate - nut connection

$$dboltn = 0.024 \text{ m}$$

$$rboltn := \frac{dboltn}{2} = 0.012 \text{ m}$$

Stress area in bottom face of steel plate A_{bottom}

$$dbottom := dboltn + 2 \cdot 3.5 \text{ mm} + 2 \cdot tf = 0.103 \text{ m}$$

$$rbottom := \frac{dbottom}{2} = 0.052 \text{ m}$$

$$A_{bottom} := 3.14 \cdot (rbottom^2 - rboltn^2) = 7.876 \times 10^{-3} \text{ m}^2$$

Stress area in bottom face of steel top A_{top}

$$dtop := dboltn + 2 \cdot 3.5 \text{ mm} = 0.031 \text{ m}$$

$$rtop := \frac{dtop}{2} = 0.016 \text{ m}$$

$$A_{top} := 3.14 \cdot (rtop^2 - rboltn^2) = 3.022 \times 10^{-4} \text{ m}^2$$

Mean Tensile Area A_{tmean}

$$A_{tmean} := \frac{A_{top} + A_{bottom}}{2} = 4.089 \times 10^{-3} \text{ m}^2$$

Maximum possible tensile capacity of plate at single nut-bot $F_{tplate1}$

$$F_{tplate1} := f_y \cdot A_{tmean} = 1.452 \times 10^6 \cdot \text{N}$$

Figure C.10: Design of 35 mm load connection part 6/9

Maximum possible tensile capacity of plate at 4 nut-bol Fplate4

$$F_{\text{plate4}} := 4 \cdot F_{\text{plate1}} = 5.806 \times 10^6 \cdot \text{N}$$

Shear Strength verification



$$r_{\text{shear}} := r_{\text{boltm}} + 3.5 \text{ mm} + \frac{t_f}{2} = 0.034 \text{ m}$$

Shear Area

$$A_{\text{shearm}} := 2 \cdot 3.14 \cdot r_{\text{shear}} \cdot t_f = 7.574 \times 10^{-3} \text{ m}^2$$

Shear capacity of a single nut Fshear1

$$F_{\text{shear1}} := f_{\text{shear}} \cdot A_{\text{shearm}} = 1.613 \times 10^6 \cdot \text{N}$$

Shear capacity of a 4 nuts Fshear4

$$F_{\text{shear4}} := 4 \cdot F_{\text{shear1}} = 6.453 \times 10^6 \cdot \text{N}$$

Figure C.11: Design of 35 mm load connection part 7/9

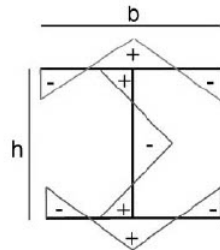
Verification for the residual stresses can occur at the web-flange section.
Reference -Instabilities of cellular members loaded in bending or compression by D. Sonck et al.

Minimum thickness when hot-rolling

$$t_{min} := t_w = 19 \cdot \text{mm}$$

Assume the maximum load per single section

$$F_{app1} := F_{t3Rd} = 904.32 \cdot \text{kN}$$



Additional Tensile stress due to residual stress at the joint

$$f_{residual} := 0.3 \cdot f_y = 106.5 \cdot \text{MPa}$$

Figure C.12: Design of 35 mm load connection part 8/9

Tensile residual force at the joint. Take the length along the joint

$$\mathbf{F_{residual}} := \mathbf{tmin} \cdot 300\mathbf{mm} \cdot \mathbf{f_{residual}} = 6.071 \times 10^5 \cdot \mathbf{N}$$

Total applied force with residual force

$$\mathbf{F_{tot}} := \mathbf{F_{app1}} + \mathbf{F_{residual}} = 1.511 \times 10^3 \cdot \mathbf{kN}$$

Tensile strength of the section. Take the length along the joint. Not at the weakest part where the shjkel hole is located

$$\mathbf{F_{max1}} := \mathbf{tmin} \cdot 300\mathbf{mm} \cdot \mathbf{f_y} = 2.023 \times 10^3 \cdot \mathbf{kN}$$

The strength is higher than the maximum applied load.

Figure C.13: Design of 35 mm load connection part 9/9

Design calculation of the New loading connection at IKM test

HEB S355 1000

Section Properties of single element (Highlighted part)

Sectional properties
of HEB section

$t_w := 19\text{mm}$
 $t_f := 36\text{mm}$
 $h_w := 450\text{mm}$
 $l_f := 300\text{mm}$

Yield Strength of web and flange

$f_y := 355 \frac{\text{N}}{\text{mm}^2}$ EN1993 1.1 Table 3.1

Yield Strength of bolt section

$f_{ybolt} := 500 \frac{\text{N}}{\text{mm}^2}$ Bolt is the threaded
reinforcement

All the marked dimensions are in
mm

Resistance of T-Stub - Step 1A

$n := 76\text{mm}$ $m_1 := 34.5\text{mm}$ EN1993 1.8 Table 6.2

$e_1 := 76\text{mm}$ EN1993 1.8 Table 6.4 and
 $d_w := 41.6\text{mm}$ M24 nut properties end to end
 diameter of nut

For a circular failure pattern

End $l_{eff1} := 2 \cdot 3.14 \cdot m_1 = 216.66 \cdot \text{mm}$ EN1993 1.8 Table 6.4
 bolt $l_{eff11} := 3.14m_1 + 2 \cdot e_1 = 260.33 \cdot \text{mm}$ (Unstiffened case)

For a non-circular failure pattern

End $l_{eff2} := 4 \cdot m_1 + 1.25 \cdot n = 0.233 \text{ m}$
 bolt $l_{eff22} := 2m_1 + 0.625 \cdot e_1 + e_1 = 0.193 \text{ m}$

Figure C.14: Design of 60 mm load connection part 1/9

$$ew := \frac{dw}{4} = 0.01 \text{ m}$$

$$\gamma_{M0} := 1 \quad \text{EN1993 1.1 NA.2.15}$$

$$\gamma_{M1} := 1$$

$$dboltm := \frac{(24.84\text{mm} + 23.16\text{mm})}{2} = 0.024 \text{ m}$$

$$FtRd := 3.14 \cdot \left(\frac{dboltm}{2}\right)^2 \cdot fybolt = 226.08 \cdot \text{kN} \quad \text{EN1993 1.8 Table 6.2 (Design resistance for T-stub flange)}$$

$$Mpl1Rd := \frac{0.25 \cdot leff1 \cdot tf^2 \cdot fy}{\gamma_{M0}} = 2.492 \times 10^4 \cdot \text{m} \cdot \text{N} \quad \text{Lesser of leff1 or leff11}$$

$$Mpl2Rd := \frac{0.25 \cdot leff2 \cdot tf^2 \cdot fy}{\gamma_{M0}} = 2.214 \times 10^4 \cdot \text{m} \cdot \text{N} \quad \text{Lesser of leff2 or leff22}$$

Mode 1 failure - Complete flange yielding

$$Ft1Rd := \frac{(8 \cdot n - 2ew) \cdot Mpl1Rd}{2 \cdot m1 \cdot n - ew \cdot (m1 + n)} = 3.574 \times 10^6 \cdot \text{m}^{-1} \cdot \text{N} \cdot \text{m}$$

Mode 2 Failure - Bolt failure with flange yielding

$$Ft2Rd := \frac{2 \cdot Mpl2Rd + n \cdot FtRd \cdot 4}{m1 + n} = 1.023 \times 10^6 \cdot \text{m}^{-1} \cdot \text{N} \cdot \text{m}$$

Mode 3 Failure - Bolt Failure

$$Ft3Rd := 4 \cdot FtRd = 9.043 \times 10^5 \cdot \text{N}$$

Resistance of flange

Minimum of Ft1Rd, Ft2Rd, Ft3Rd

$$Ft3Rd = 9.043 \times 10^5 \cdot \text{N}$$

Figure C.15: Design of 60 mm load connection part 2/9

Check for Beam Web tension - Step 1B

EN1993 1.8 Section 6.2.6.8

$$b_{effweb} := 300\text{mm} - 86\text{mm} = 0.214\text{m}$$

EN1993 1.8 Section 6.2.6.8 suggest to use Fig.6.10 and Table 6.6

$$t_{wb} := t_w = 19 \cdot \text{mm}$$

Consider the combined section

$$f_{ywb} := 355 \frac{\text{N}}{\text{mm}^2}$$

Web tensile Capacity

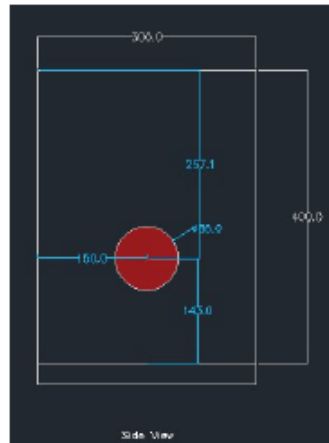
$$F_{twbRd} := \frac{b_{effweb} \cdot t_{wb} \cdot f_{ywb}}{\gamma_{M0}} = 1.443 \times 10^3 \cdot \text{kN}$$

EN1993 1.8 in Eq 6.22

Shear failure can occur at the loading shackle connection

Ref:

<https://www.machinedesign.com/fasteners/what-s-difference-between-bearing-shear-and-tear-out-stress>



$$A_{shear} := 2 \cdot 257\text{mm} \cdot t_w = 9.766 \times 10^{-3} \text{m}^2$$

Figure C.16: Design of 60 mm load connection part 3/9

$$f_{\text{shear}} := 0.6 \cdot f_{ywb} = 2.13 \times 10^8 \frac{\text{N}}{\text{m}^2}$$

$$F_{\text{shearRD}} := A_{\text{shear}} \cdot f_{\text{shear}} = 2.08 \times 10^6 \text{ Pa}$$

Tearout Failure of web

Ref:

<https://www.machinedesign.com/fasteners/what-s-difference-between-bearing-shear-and-tear-out-stress>

To prevent tear-out, it is suggested that the distance from the edge of the material to the edge of the hole be at least equal to the diameter of the hole

Therefore No tearout fail occur

Verification of nut and bolt connection

Nut Strength Verification

The bolt is considered as the threaded end of reinforcement and the nut is selected as M24 strength class 8.

Tensile strength of 4 bolt set

$$F_{t3Rd} = 9.043 \times 10^5 \text{ N}$$

Refer sheet No.2

Verification for the thread stripping before tensile failure of bolts

Tensile strength of one bolt

$$F_{\text{bolt}} := \frac{F_{t3Rd}}{4} = 2.261 \times 10^5 \text{ N}$$

Figure C.17: Design of 60 mm load connection part 4/9

Shear strength of bolt from the reinforcement

$$F_{\text{shearbolt}} := 0.85 \cdot f_{y\text{bolt}} = 425 \cdot \text{MPa}$$

0.85 is the EC2 factor used when calculating shear links

Calculation of effective length

$$A_{\text{shearbolt}} := \frac{F_{\text{bolt}}}{F_{\text{shearbolt}}} = 5.32 \times 10^{-4} \text{ m}^2$$

$$L_{\text{effshear}} := \frac{A_{\text{shearbolt}}}{3.14 \cdot d_{\text{boltm}}} = 7.059 \times 10^{-3} \text{ m}$$

In order to hold the Tensile strength of a bolt required length is

$$L_{\text{effshear}} = 7.059 \times 10^{-3} \text{ m}$$

Reference
www.tribology-abc.com

http://www.tribology-abc.com/calculators/e3_6e.htm

Thread stripping strength of bolt (reinforcement) $F_{\text{threadbolt}}$

Reference :
<http://www.tribology-abc.com/sub9.htm>

Length of engagement

$$L_{\text{eng}} := 0.75 \cdot 24\text{mm} = 0.018 \text{ m}$$

Assume only one nut is used

$$A_{\text{engshear}} := 3.14 \cdot d_{\text{boltm}} \cdot L_{\text{eng}} = 1.356 \times 10^{-3} \text{ m}^2$$

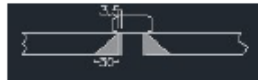
$$F_{\text{threadbolt}} := A_{\text{engshear}} \cdot F_{\text{shearbolt}} = 5.765 \times 10^5 \cdot \text{N}$$

Thread stripping does not occur before Tensile strength of bolt

Figure C.18: Design of 60 mm load connection part 5/9

Verification for the thickness of flange (steel plate connected to bolts)

Tensile Strength verification



cross section of steel plate - nut connection

$$d_{boltm} = 0.024 \text{ m}$$

$$r_{boltm} := \frac{d_{boltm}}{2} = 0.012 \text{ m}$$

Stress area in bottom face of steel plate A_{bottom}

$$d_{bottom} := d_{boltm} + 2 \cdot 3.5 \text{ mm} + 2 \cdot t_f = 0.103 \text{ m}$$

$$r_{bottom} := \frac{d_{bottom}}{2} = 0.052 \text{ m}$$

$$A_{bottom} := 3.14 \cdot (r_{bottom}^2 - r_{boltm}^2) = 7.876 \times 10^{-3} \text{ m}^2$$

Stress area in bottom face of steel top A_{top}

$$d_{top} := d_{boltm} + 2 \cdot 3.5 \text{ mm} = 0.031 \text{ m}$$

$$r_{top} := \frac{d_{top}}{2} = 0.016 \text{ m}$$

$$A_{top} := 3.14 \cdot (r_{top}^2 - r_{boltm}^2) = 3.022 \times 10^{-4} \text{ m}^2$$

Mean Tensile Area A_{tmean}

$$A_{tmean} := \frac{A_{top} + A_{bottom}}{2} = 4.089 \times 10^{-3} \text{ m}^2$$

Maximum possible tensile capacity of plate at single nut-bot $F_{tplate1}$

$$F_{tplate1} := f_y \cdot A_{tmean} = 1.452 \times 10^6 \cdot \text{N}$$

Figure C.19: Design of 60 mm load connection part 6/9

Maximum possible tensile capacity of plate at 4 nut-bol F_{plate4}

$$\mathbf{F_{plate4} := 4 \cdot F_{plate1} = 5.806 \times 10^6 \cdot N}$$

Shear Strength verification



$$\mathbf{r_{shear} := r_{boltm} + 3.5\text{mm} + \frac{tf}{2} = 0.034\text{m}}$$

Shear Area

$$\mathbf{A_{shearm} := 2 \cdot 3.14 \cdot r_{shear} \cdot tf = 7.574 \times 10^{-3} \text{m}^2}$$

Shear capacity of a single nut F_{shear1}

$$\mathbf{F_{shear1} := f_{shear} \cdot A_{shearm} = 1.613 \times 10^6 \cdot N}$$

Shear capacity of a 4 nuts F_{shear4}

$$\mathbf{F_{shear4} := 4 \cdot F_{shear1} = 6.453 \times 10^6 \cdot N}$$

Figure C.20: Design of 60 mm load connection part 7/9

Verification for the residual stresses can occur at the web-flange section.

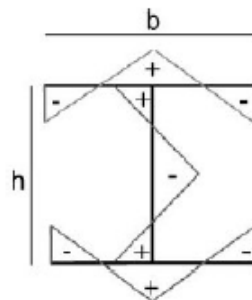
Reference -Instabilities of cellular members loaded in bending or compression by D. Sonck et al.

Minimum thickness when hot-rolling

$$t_{min} := fw - 19 \cdot mm$$

Assume the maximum load per single section

$$F_{appl} := Ft3Rd = 904.32 \cdot kN$$



Additional Tensile stress due to residual stress at the joint

$$f_{residual} := 0.3 \cdot fy = 106.5 \cdot MPa$$

Figure C.21: Design of 60 mm load connection part 8/9

Tensile residual force at the joint. Take the length along the joint

$$\mathbf{F_{residual} := t_{min} \cdot 300\text{mm} \cdot f_{residual} = 6.071 \times 10^5 \cdot \mathbf{N}}$$

Total applied force with residual force

$$\mathbf{F_{tot} := F_{appl} + F_{residual} = 1.511 \times 10^3 \cdot \mathbf{kN}}$$

Tensile strength of the section. Take the length along the joint. Not at the weakest part where the shjake hole is located

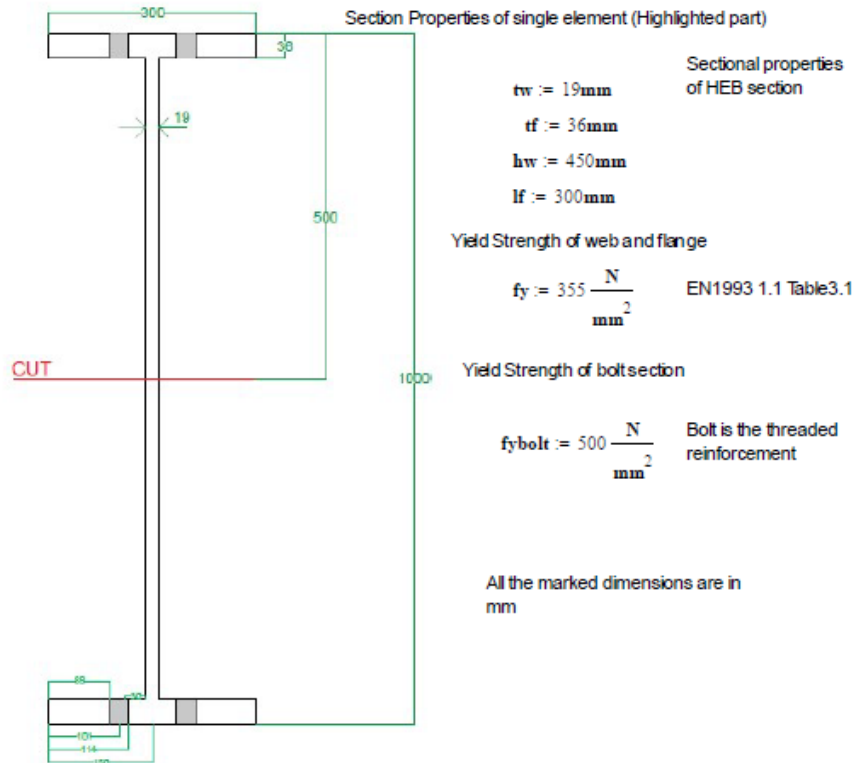
$$\mathbf{F_{max1} := t_{min} \cdot 300\text{mm} \cdot f_y = 2.023 \times 10^3 \cdot \mathbf{kN}}$$

The strength is higher than the maximum applied load.

Figure C.22: Design of 60 mm load connection part 9/9

Design calculation of the New loading connection at IKM test

HEB S355 1000



Resistance of T-Stubs - Step 1A

$n := 101 \text{ mm}$ $m1 := 9.5 \text{ mm}$ EN1993 1.8 Table 6.2

$e1 := 101 \text{ mm}$ EN1993 1.8 Table 6.4 and M24 nut properties end to end diameter of nut

$dw := 41.6 \text{ mm}$

For a circular failure pattern

End $leff1 := 2 \cdot 3.14 \cdot m1 = 59.66 \cdot \text{mm}$ EN1993 1.8 Table 6.4 (Unstiffened case)

bolt $leff11 := 3.14m1 + 2 \cdot e1 = 231.83 \cdot \text{mm}$

For a non-circular failure pattern

End $leff2 := 4 \cdot m1 + 1.25 \cdot n = 0.164 \text{ m}$

bolt $leff22 := 2m1 + 0.625 \cdot e1 + e1 = 0.183 \text{ m}$

Figure C.23: Design of 85 mm load connection part 1/9

$$e_w := \frac{d_w}{4} = 0.01 \text{ m}$$

$$\gamma_{M0} := 1 \quad \text{EN1993 1.1 NA2.15}$$

$$\gamma_{M1} := 1$$

$$d_{boltm} := \frac{(24.84\text{mm} + 23.16\text{mm})}{2} = 0.024 \text{ m}$$

$$F_{tRd} := 3.14 \cdot \left(\frac{d_{boltm}}{2} \right)^2 \cdot f_{ybolt} = 226.08 \cdot \text{kN} \quad \text{EN1993 1.8 Table 6.2 (Design resistance for T-stub flange)}$$

$$M_{pl1Rd} := \frac{0.25 \cdot l_{eff1} \cdot t_f^2 \cdot f_y}{\gamma_{M0}} = 6.862 \times 10^3 \text{ m} \cdot \text{N} \quad \text{Lesser of } l_{eff1} \text{ or } l_{eff11}$$

$$M_{pl2Rd} := \frac{0.25 \cdot l_{eff2} \cdot t_f^2 \cdot f_y}{\gamma_{M0}} = 1.889 \times 10^4 \cdot \text{N} \cdot \text{m} \quad \text{Lesser of } l_{eff2} \text{ or } l_{eff22}$$

Mode 1 failure -Complete flange yielding

$$F_{t1Rd} := \frac{(8 \cdot n - 2e_w) \cdot M_{pl1Rd}}{2 \cdot m1 \cdot n - e_w \cdot (m1 + n)} = 7.017 \times 10^6 \text{ m}^{-1} \cdot \text{N} \cdot \text{m}$$

Mode 2 Failure - Bolt failure with flange yielding

$$F_{t2Rd} := \frac{2 \cdot M_{pl2Rd} + n F_{tRd} \cdot 4}{m1 + n} = 1.169 \times 10^6 \text{ m}^{-1} \cdot \text{N} \cdot \text{m}$$

Mode3 Failure - Bolt Failure

$$F_{t3Rd} := 4 \cdot F_{tRd} = 9.043 \times 10^5 \cdot \text{N}$$

Resistance of flange

Minimum of F_{t1Rd} , F_{t2Rd} , F_{t3Rd}

$$F_{t3Rd} = 9.043 \times 10^5 \cdot \text{N}$$

Figure C.24: Design of 85 mm load connection part 2/9

Check for Beam Web tension - Step 1B

EN1993 1.8 Section 6.2.6.8

$$b_{effweb} := 300\text{mm} - 86\text{mm} = 0.214\text{m}$$

EN1993 1.8 Section 6.2.6.8 suggest to use Fig.6.10 and Table 6.6

$$t_{wb} := t_w = 19\text{mm}$$

Consider the combined section

$$f_{ywb} := 355 \frac{\text{N}}{\text{mm}^2}$$

Web tensile Capacity

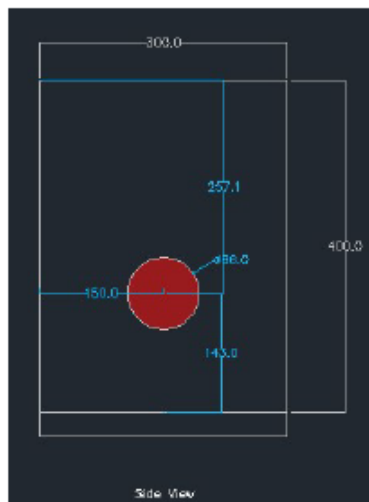
$$F_{twbRd} := \frac{b_{effweb} \cdot t_{wb} \cdot f_{ywb}}{\gamma M 0} = 1.443 \times 10^3 \cdot \text{kN}$$

EN1993 1.8 in Eq 6.22

Shear failure can occur at the loading shackle connection

Ref:

<https://www.machinedesign.com/fasteners/what-s-difference-between-bearing-shear-and-tear-out-stress>



$$A_{shear} := 2 \cdot 257\text{mm} \cdot t_w = 9.766 \times 10^{-3} \text{m}^2$$

Figure C.25: Design of 85 mm load connection part 3/9

$$f_{\text{shear}} := 0.6 \cdot f_{ywb} = 2.13 \times 10^8 \frac{\text{N}}{\text{m}^2}$$

$$F_{\text{shearRD}} := A_{\text{shear}} \cdot f_{\text{shear}} = 2.08 \times 10^6 \text{ m}^2 \cdot \text{Pa}$$

Tearout Failure of web

Ref:

<https://www.machinedesign.com/fasteners/what-s-difference-between-bearing-shear-and-tear-out-stress>

To prevent tear-out, it is suggested that the distance from the edge of the material to the edge of the hole be at least equal to the diameter of the hole

Therefore No tearout fail occur

Verification of nut and bolt connection

Nut Strength Verification

The bolt is considered as the threaded end of reinforcement and the nut is selected as M24 strength class 8.

Tensile strength of 4 bolt set

$$F_{t3Rd} = 9.043 \times 10^5 \cdot \text{N}$$

Refer sheet No.2

Verification for the thread stripping before tensile failure of bolts

Tensile strength of one bolt

$$F_{\text{bolt}} := \frac{F_{t3Rd}}{4} = 2.261 \times 10^5 \cdot \text{N}$$

Figure C.26: Design of 85 mm load connection part 4/9

Shear strength of bolt from the reinforcement

$$F_{\text{shearbolt}} := 0.85 \cdot f_{y\text{bolt}} = 425 \cdot \text{MPa}$$

0.85 is the EC2 factor used when calculating shear links

Calculation of effective length

$$A_{\text{shearbolt}} := \frac{F_{\text{bolt}}}{F_{\text{shearbolt}}} = 5.32 \times 10^{-4} \cdot \text{m}^2$$

$$L_{\text{effshear}} := \frac{A_{\text{shearbolt}}}{3.14 \cdot d_{\text{boltm}}} = 7.059 \times 10^{-3} \cdot \text{m}$$

In order to hold the Tensile strength of a bolt required length is

$$L_{\text{effshear}} = 7.059 \times 10^{-3} \cdot \text{m}$$

Reference
www.tribology-abc.com

http://www.tribology-abc.com/calculators/e3_6e.htm

Thread stripping strength of bolt (reinforcement) $F_{\text{threadbolt}}$

Reference :
<http://www.tribology-abc.com/sub9.htm>

Length of engagement

$$L_{\text{eng}} := 0.75 \cdot 24\text{mm} = 0.018 \cdot \text{m}$$

Assume only one nut is used

$$A_{\text{engshear}} := 3.14 \cdot d_{\text{boltm}} \cdot L_{\text{eng}} = 1.356 \times 10^{-3} \cdot \text{m}^2$$

$$F_{\text{threadbolt}} := A_{\text{engshear}} \cdot F_{\text{shearbolt}} = 5.765 \times 10^5 \cdot \text{N}$$

Thread stripping does not occur before Tensile strength of bolt

Figure C.27: Design of 85 mm load connection part 5/9

Verification for the thickness of flange (steel plate connected to bolts)

Tensile Strength verification



cross section of steel plate - nut connection

$$dboltm = 0.024 \text{ m}$$

$$rboltm := \frac{dboltm}{2} = 0.012 \text{ m}$$

Stress area in bottom face of steel plate A_{bottom}

$$dbottom := dboltm + 2 \cdot 3.5\text{mm} + 2 \cdot tf = 0.103 \text{ m}$$

$$rbottom := \frac{dbottom}{2} = 0.052 \text{ m}$$

$$A_{bottom} := 3.14 \cdot (rbottom^2 - rboltm^2) = 7.876 \times 10^{-3} \text{ m}^2$$

Stress area in bottom face of steel top A_{top}

$$dtop := dboltm + 2 \cdot 3.5\text{mm} = 0.031 \text{ m}$$

$$rtop := \frac{dtop}{2} = 0.016 \text{ m}$$

$$A_{top} := 3.14 \cdot (rtop^2 - rboltm^2) = 3.022 \times 10^{-4} \text{ m}^2$$

Mean Tensile Area A_{tmean}

$$A_{tmean} := \frac{A_{top} + A_{bottom}}{2} = 4.089 \times 10^{-3} \text{ m}^2$$

Maximum possible tensile capacity of plate at single nut-bol $F_{tplate1}$

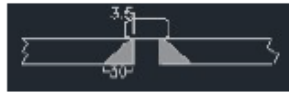
$$F_{tplate1} := fy \cdot A_{tmean} = 1.452 \times 10^6 \cdot \text{N}$$

Figure C.28: Design of 85 mm load connection part 6/9

Maximum possible tensile capacity of plate at 4 nut-bolts $F_{tplate4}$

$$F_{tplate4} := 4 \cdot F_{tplate1} = 5.806 \times 10^6 \cdot N$$

Shear Strength verification



$$r_{shear} := r_{boltm} + 3.5\text{mm} + \frac{tf}{2} = 0.034 \text{ m}$$

Shear Area

$$A_{shearm} := 2 \cdot 3.14 \cdot r_{shear} \cdot tf = 7.574 \times 10^{-3} \text{ m}^2$$

Shear capacity of a single nut F_{shear1}

$$F_{shear1} := f_{shear} \cdot A_{shearm} = 1.613 \times 10^6 \cdot N$$

Shear capacity of 4 nuts F_{shear4}

$$F_{shear4} := 4 \cdot F_{shear1} = 6.453 \times 10^6 \cdot N$$

Figure C.29: Design of 85 mm load connection part 7/9

Verification for the residual stresses can occur at the web-flange section.

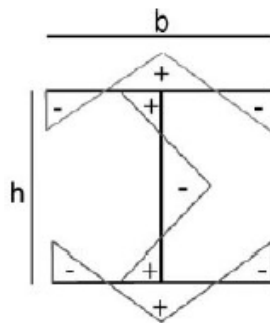
Reference -Instabilities of cellular members loaded in bending or compression by D. Sonck et al.

Minimum thickness when hot-rolling

$$t_{min} := t_w = 19 \cdot \text{mm}$$

Assume the maximum load per single section

$$F_{app1} := F_t3R_d = 904.32 \cdot \text{kN}$$



Additional Tensile stress due to residual stress at the joint

$$f_{residual} := 0.3 \cdot f_y = 106.5 \cdot \text{MPa}$$

Figure C.30: Design of 85 mm load connection part 8/9

Tensile residual force at the joint. Take the length along the joint

$$F_{\text{residual}} := t_{\text{min}} \cdot 300 \text{ mm} \cdot f_{\text{residual}} = 6.071 \times 10^5 \cdot \text{N}$$

Total applied force with residual force

$$F_{\text{tot}} := F_{\text{appl}} + F_{\text{residual}} = 1.511 \times 10^3 \cdot \text{kN}$$

Tensile strength of the section. Take the length along the joint. Not at the weakest part where the shjake hole is located

$$F_{\text{max1}} := t_{\text{min}} \cdot 300 \text{ mm} \cdot f_y = 2.023 \times 10^3 \cdot \text{kN}$$

The strength is higher than the maximum applied load.

Figure C.31: Design of 85 mm load connection part 9/9

D Images of cracks in concrete

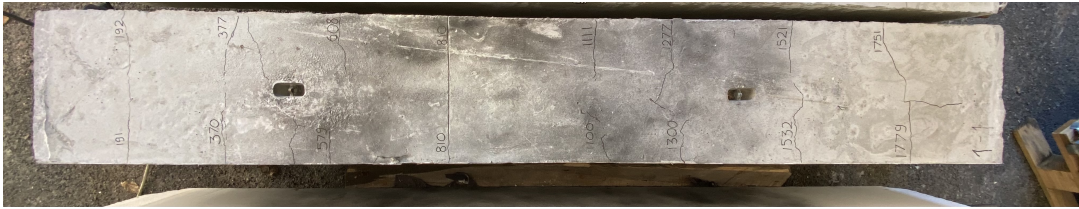


Figure D.1: Beam 1 - Side 1

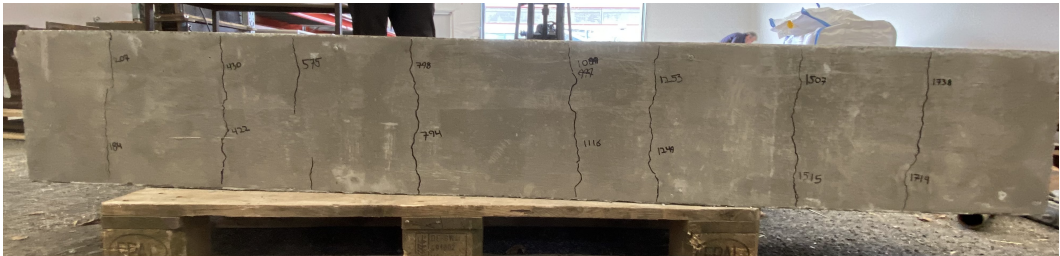


Figure D.2: Beam 1 - Side 2

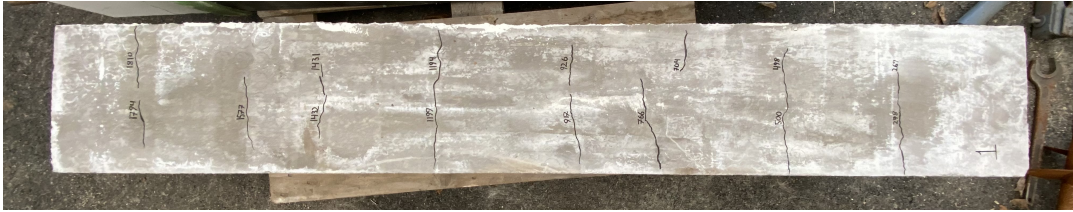


Figure D.3: Beam 1 - Side 3



Figure D.4: Beam 1 - Side 4



Figure D.5: Beam 2 - Side 1



Figure D.6: Beam 2 - Side 1

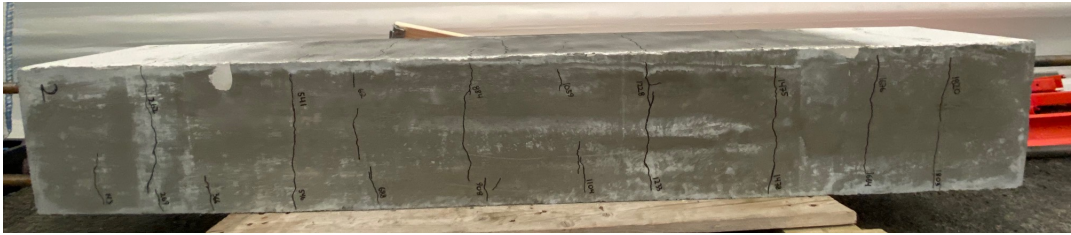


Figure D.7: Beam 2 - Side 3



Figure D.8: Beam 2 - Side 4

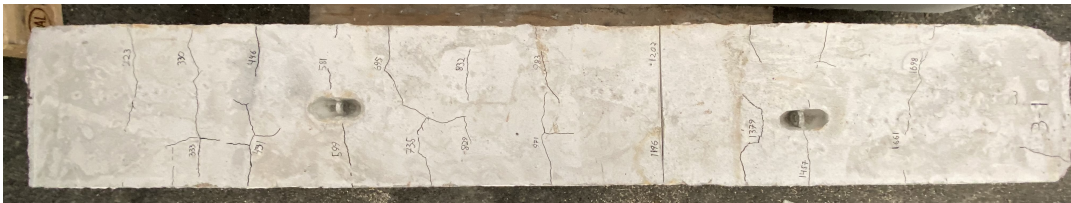


Figure D.9: Beam 3 - Side 1



Figure D.10: Beam 3 - Side 2



Figure D.11: Beam 3 - Side 3

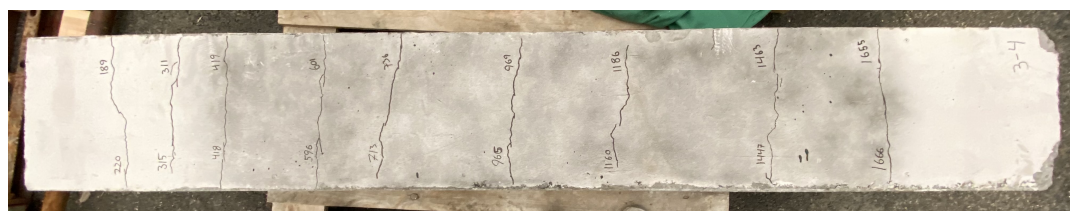


Figure D.12: Beam 3 - Side 4

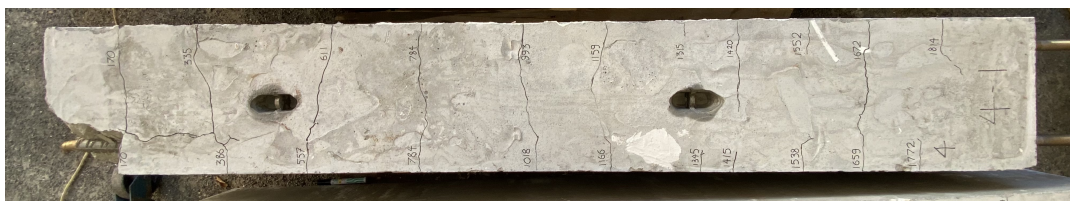


Figure D.13: Beam 4 - Side 1

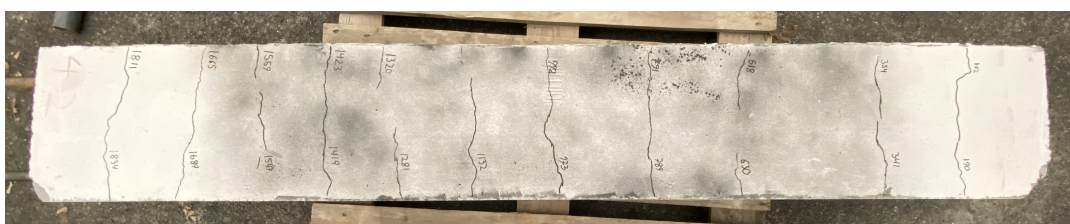


Figure D.14: Beam 4 - Side 2



Figure D.15: Beam 4 - Side 3

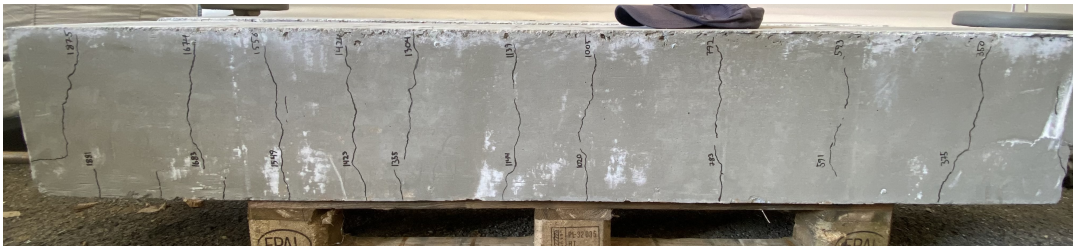


Figure D.16: Beam 4 - Side 4

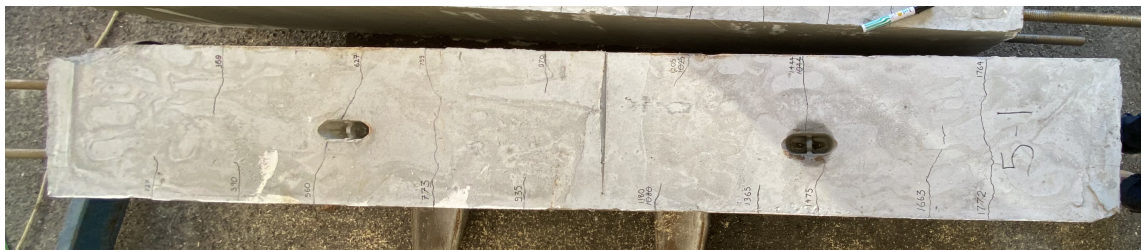


Figure D.17: Beam 5 - Side 1



Figure D.18: Beam 5 - Side 2



Figure D.23: Beam 6 - Side 3

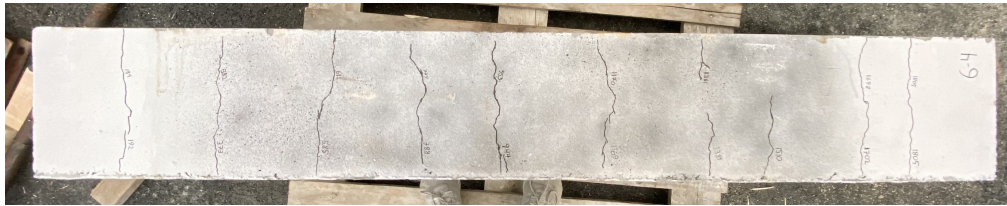


Figure D.24: Beam 6 - Side 4